Article

Lacunicambarus chimera: a new species of burrowing crayfish (Decapoda: Cambaridae) from Illinois, Indiana, Kentucky, and Tennessee

MAEL G. GLON[1,3], ROGER F. THOMA[2], MARYMEGAN DALY[1] & JOHN V. FREUDENSTEIN[1]

[1]*The Ohio State University Museum of Biological Diversity, 1315 Kinnear Road, Columbus, Ohio 43212, USA*
[2]*Midwest Biodiversity Institute, 4673 Northwest Parkway, Hilliard, Ohio 43026, USA*
[3]*Corresponding author. E-mail: glon.1@osu.edu*

Abstract

Lacunicambarus diogenes (Girard 1852) was, until recently, considered to be one of the most widely distributed North American crayfish species, occurring in 31 U.S. States and one Canadian province east of the North American Rocky Mountains. Glon *et al.* (2018) investigated this claim and found that *L. diogenes* sensu lato was actually a species complex. The authors redescribed *L. diogenes* and restricted its range to the Atlantic Coastal Plain and Piedmont ecoregions of eastern North America. In doing so, they also revealed the existence of several probable undescribed species of *Lacunicambarus* that were previously considered to be *L. diogenes*. Here, we use morphological and molecular techniques to distinguish and describe one of these species: *Lacunicambarus chimera* **sp. nov.**, a large primary burrowing crayfish found in parts of the Lower Mississippi, Ohio, Tennessee and Upper Mississippi River Basins. *Lacunicambarus chimera* is morphologically similar to *L. diogenes*, from which it can be distinguished by the greater number of spines on the ventrolateral margin of its merus, its wider antennal scale terminating in a short spine, and the presence of a single longitudinal stripe on the dorsal side of its abdomen. We also provide an updated key to *Lacunicambarus*.

Key words: burrowing crayfish, systematics, taxonomy, revision, North America, freshwater, Old Ohio River

Introduction

The North American crayfish family Cambaridae Hobbs 1942 comprises approximately two-thirds (> 400) of global crayfish species (Taylor *et al.* 2007, Richman *et al.* 2015; Crandall & De Grave 2017). Despite this already impressive number, new species of North American crayfishes have continued to be discovered and described in recent decades due to heightened interest in crayfish taxonomy and increased availability and sophistication of molecular phylogenetic techniques. Such techniques are particularly useful in efforts to tease apart species complexes, which have long plagued North American crayfish taxonomy (e.g., Ainscough *et al.* 2013; Thoma *et al.* 2016; Loughman *et al.* 2017).

One such complex is the devil crayfish species complex. The devil crayfish, *Lacunicambarus diogenes* (Girard 1852), was first described as *Cambarus diogenes* from "the neighborhoods of the City of Washington." The account of morphology in the original description was vague, and the type specimen of the species was lost in the Great Chicago Fire of 1871 (Faxon 1885). As a result of these circumstances, several subsequent astacologists expressed skepticism that *L. diogenes* was a single species, but it proved difficult to further unravel this species complex (e.g., Faxon 1885; Ortmann 1906; Hobbs 1981; Jezerinac 1993). The documented range of this species therefore gradually increased until it became one of the most widely distributed crayfishes in North America, occurring in 31 U.S. states and one Canadian province east of the North American Rocky Mountains (Taylor *et al.* 2007).

Glon *et al.* (2018) used molecular phylogenetic techniques to analyze a large number of specimens from across the range of the devil crayfish species complex. The authors found that the complex as a whole formed a clade distinct from *Cambarus* Erichson 1846 and therefore elevated the subgenus *Lacunicambarus* Hobbs 1969 (which originally included *L. diogenes*) to generic rank and amended its description to also encompass species that had

previously been in the subgenus *Tubericambarus* Jezerinac 1993. Additionally, the authors redescribed *L. diogenes*, designated a neotype for the species, and restricted its range to the Atlantic Coastal Plain and Piedmont ecoregions of eastern North America, from New Jersey in the north to Georgia in the south.

Although these taxonomic acts resolved part of the disarray surrounding this species complex, they also revealed the existence of several probable undescribed species of *Lacunicambarus* previously considered to be *L. diogenes*. Here, we take a next step towards a systematic revision of *Lacunicambarus* by describing one of these species: *Lacunicambarus chimera* **sp. nov.** We first encountered this species in Kentucky during the summer of 2017 while searching for a population of very large crayfish, members of which were nicknamed "Crawzilla" by Raymond F. Jezerinac and Whitney G. Stocker in the 1980s. It remains unclear to us whether this species is the same that these astacologists first encountered, but we feel that its impressive size makes it worthy of such a name.

Methods

Sampling. We used both museum and freshly-collected specimens in our analyses (Tables 1, 2). In 2017 and 2018, we collected fresh specimens from burrows in Illinois, Indiana, Kentucky, and Tennessee which we excavated by hand or with a small gardening pickaxe or shovel. Shortly following capture, we used sterilized forceps to remove gill tissue from each specimen, which we preserved in tubes of 100% ethanol and froze (-20 °C) as soon as possible for subsequent molecular analyses. We preserved voucher specimens in jars of 70% ethanol and later catalogued and deposited them in the crustacean collection of the Ohio State University Museum of Biological Diversity (OSUMC). We obtained additional preserved specimens for our analyses from OSUMC and the Smithsonian National Museum of Natural History (USNM).

Molecular analyses. Our molecular analysis protocol directly followed the methods outlined in Glon *et al.* (2018). Briefly, we extracted total genomic DNA from gill tissue samples using a DNeasy Blood and Tissue Kit (Qiagen, Hilden, Germany), then used PCR to amplify three mitochondrial loci: partial 12S, partial 16S and partial CO1. We sent aliquots of our PCR products to TacGen (Richmond, California, USA) for sequencing in both directions on an ABI 3730XL DNA analyzer using BigDye Terminator v3.1 sequencing chemistry. We downloaded additional *Lacunicambarus* sequences generated by Glon *et al.* (2018) from GenBank and included these in our analyses (see Glon *et al.* 2018 Supplementary Material Table S1 for specimen data and GenBank accession numbers). We assembled our sequences and performed MUSCLE alignments (Edgar 2004) for each locus in Geneious R11 (www.geneious.com; Kearse *et al.* 2012). We uploaded all newly generated sequences to GenBank (Table 2). We used jModelTest 2 (Darriba *et al.* 2012; Guindon & Gascuel 2003) with three substitution schemes to compute likelihood scores for 24 candidate nucleotide substitution models and performed model selection using the Akaike Information Criterion corrected for small sample size (AICc) and the Bayesian Information Criterion (BIC). We partitioned our aligned sequences by locus and designated substitution models for each partition based on the results of jModelTest 2. We inferred phylogenetic trees and established nodal support using Maximum Likelihood with bootstrap in IQ-Tree (Nguyen *et al.* 2015; Chernomor *et al.* 2016) and Bayesian inference with Markov-Chain Monte Carlo in MrBayes (Huelsenbeck & Ronquist 2001; Ronquist & Huelsenbeck 2003).

Morphometric and meristic analyses. *Lacunicambarus chimera* was previously lumped into the *L. diogenes* species complex as a result of Girard's (1852) vague description. Using molecular phylogenetic techniques, Glon *et al.* (2018) demonstrated that this species complex was an agglomeration of multiple species, one of which was *L. chimera*. However, we feel that it is important to be able to distinguish crayfish species using techniques other than molecular phylogenetics whenever feasible and to verify the results of molecular analyses, so we used morphometric and meristic analyses to elucidate characters that differ between *L. chimera* and *L. diogenes.*

We measured morphometric and meristic characters from 50 specimens each of *L. chimera* and *L. diogenes* using digital calipers (accurate to the nearest 0.01 mm) and a dissecting microscope. We only analyzed data from undamaged adult specimens with at least one original chela (n = 98). From these measurements, we calculated the following 14 ratios, adapted from Fetzner & Taylor (2018) and Loughman & Williams (2018): carapace width/length, carapace depth/length, areola length/carapace length, cephalon width/length, postorbital ridge width/cephalon width, rostrum width at eyes/rostrum length, rostrum length/cephalon length, acumen length/width, antennal scale length/width, palm length/propodus length, palm length/width, palm depth/propodus length, dactyl length/propodus length. We also obtained the following meristic characters: number of cervical tubercles, number

of anteroventral branchiostegal tubercles, number of spines of both the ventromesial and ventrolateral margins of the merus, and number of tubercles on the mesial margin of the dactyl. Lastly, we calculated three ratios for male specimens only (gonopod umbo width/gonopod length, central projection length/gonopod length, mesial process length/gonopod length) and one ratio for female specimens only (annulus ventralis length/width).

We analyzed our data as a whole (n = 49 of each species), then partitioned into Form I males (n = 10, *L. chimera*; n = 17, *L. diogenes*), Form II males (n = 16, *L. chimera*; n = 9, *L. diogenes*), and females (n = 23 of each species). For each partition, we used Shapiro-Wilk tests to test for normality of each morphometric and meristic character, then correspondingly used either Welch's t-test or the non-parametric Wilcoxon Rank-Sum Test to test the null hypothesis of equal means between species. In order to account for the increased risk of Type I error associated with multiple tests, we used a Bonferroni correction to adjust our p-values according to the number of tests performed per partition of our data (Table 3). We eliminated from subsequent multivariate analyses those variables that were not significantly different between species after Bonferroni correction.

We performed non-metric multidimensional scaling (NMDS) using the function metaMDS from the Vegan package (Oksanen *et al.* 2018) on each of our partitions to scale the matrix of morphometric ratios and meristic characters down to two-dimensions. These analyses were based on a Bray-Curtis distance matrix and were run for a maximum of 500 iterations. We considered the reduced-dimension representations of our data to be acceptable if NMDS stress scores were ≤ 0.2 (McCune & Grace 2002; Fetzner & Taylor 2018). We used the packages ggord (Beck 2018) and ggplot2 (Wickham 2016) to generate NMDS plots with significant characters plotted as vectors and confidence ellipses for each species. We conducted all of our analyses in R (R Core Team 2017)

Results

Molecular analyses. Our AICc and BIC analyses in jModelTest 2 found that the most appropriate nucleotide substitution models were HKY+G for 12S and 16S and HKY+I+G for partial CO1. Our maximum likelihood tree had a log likelihood value of -7369.196. The standard deviation of the split frequencies dropped below 0.01 during our Bayesian analysis, indicating convergence. Each of our two independent MrBayes runs generated 10,001 trees, 2,500 of which were discarded as burn-in, which left 17,502 trees in our post-burnin posterior distribution. The topologies of our Maximum Likelihood (ML) and Bayesian Inference (BI) trees have no significantly supported disagreements. We therefore present our ML tree annotated with both Bayesian posterior probabilities (PP_{BI}) and ML bootstrap values (B_{ML}; Figure 1).

Both analyses found strong support for a clade consisting of all of our specimens of *L. chimera* ($PP_{BI} = 1$, $B_{ML} = 79$). Interestingly, this clade was further divided into two maximally supported clades ($PP_{BI} = 1$, $B_{ML} = 97$ and $PP_{BI} = 1$, $B_{ML} = 99$). This division corresponds loosely with a northeast to southwest cline but does not seem to be associated with any single contemporary geographical or hydrological barrier or any obvious morphological differences. Additional sampling may help elucidate this pattern, but we currently consider both of these clades to be *L. chimera*.

Morphometric and meristic analyses. For our complete dataset, nine characters were significantly different between species following the Bonferroni correction (Table 3): acumen length/width, palm length/propodus length, antennal scale length/width, palm length/width, dactyl length/propodus length, number of anteroventral branchiostegal tubercles, number of spines on both the ventromesial and ventrolateral margins of the merus, and number of tubercles on the mesial margin of the dactyl. Our NMDS converged on a two-dimensional solution with an acceptable stress level (non-metric fit $R^2 = 0.91$; linear fit $R^2 = 0.92$; stress = 0.133). *Lacunicambarus chimera* and *L. diogenes* form two clusters of points with a small amount of overlap on our NMDS plot for this partition (Figure 2)

For Form I males, seven measurements were significantly different between species following the Bonferroni correction (Table 3): gonopod umbo width/gonopod length, central projection length/gonopod length, mesial process length/gonopod length, number of anteroventral branchiostegal tubercles, number of spines on both the ventromesial and ventrolateral margins of the merus, and number of tubercles on the mesial margin of the dactyl. Our NMDS converged on a two-dimensional solution with an acceptable stress level (non-metric fit $R^2 = 0.99$; linear fit $R^2 = 0.99$; stress = 0.054). *Lacunicambarus chimera* and *L. diogenes* form two very distinct clusters of points with no overlap on our NMDS plot for this partition (Figure 3).

TABLE 1. Data on examined specimens of *Lacunicambarus chimera* sp. nov. including catalogue number, State and County of collection, collection date, number of specimens of each sex and Form, and other crayfish species found at collection sites. Asterisk denotes type locality. Abbreviations: *C.*, *Creaserinus* ; *F.*, *Faxonius* ; *L.*, *Lacunicambarus*, MGG, Mael G. Glon; *P.*, *Procambarus* ; RFT, Roger F. Thoma; USNM, Smithsonian National Museum of Natural History.

Field/catalogue #	State	County	Collection date	Form I males	Form II males	Females	Juveniles	Other species
USNM 310437	Illinois	Gallatin	1936-05-15			1		
MGG-180613-05	Illinois	Massac	2018-06-13		2	2		*C. fodiens, L.* aff *polychromatus*
MGG-180614-01	Illinois	Massac	2018-06-14		1	5		*P. acutus, C. hortoni, L. polychromatus*
MGG-180613-03	Illinois	Pulaski	2018-06-13		1	1		*C. fodiens*
USNM 149080	Illinois	Pulaski	1979-03-15	2			1	
USNM 43760	Illinois	Wabash	1881	1		1		
MGG-180614-06*	Illinois	White	2018-06-14	1	2	3		*P. gracilis, F. immunis*
USNM 1462932	Indiana	Knox	1970-12-19	1				*L. polychromatus*
MGG-170812-03	Indiana	Pike	2017-08-12		2	6	1	*L. polychromatus*
MGG-170812-03B	Indiana	Pike	2017-08-12	2	10	8	3	*L. polychromatus*
USNM 91585	Indiana	Posey	1943-06-03			1		
USNM 178476	Indiana	Vanderburgh	1982-06-12	1		1	1	
USNM 178501	Kentucky	Ballard	1982-06-12	2	1	3	1	
USNM 148711	Kentucky	Calloway	1978-03-23	1				
USNM 176307	Kentucky	Calloway	1979-05-17			1		
USNM 149052	Kentucky	Christian	1979-03-10			1	1	
USNM 220325	Kentucky	Fulton	1941-06-26	1	1	1		
MGG-180612-04	Kentucky	Graves	2018-06-12	1	2	4	1	*P. clarkii, P. viaeviridis*
USNM 177547	Kentucky	Graves	1980-02-22	1		1	2	
USNM 218865	Kentucky	Graves	1985-01-19	1				
USNM 149067	Kentucky	Hickman	1979-03-09	1		2		
MGG-180612-01	Kentucky	Hopkins	2018-06-12		3	4	2	
USNM 218102	Kentucky	Jefferson	1961-01-01	1				
USNM 218096	Kentucky	Jefferson	1963-04-12	1				
MGG-180612-03	Kentucky	Livingston	2018-06-12		1	6	1	*P. acutus*
USNM 130133	Kentucky	Marshall	1969-04-14		1		1	
RFT-17-040	Kentucky	McCracken	2017-07-31		1			
RFT-17-041	Kentucky	McCracken	2017-07-31				4	
USNM 260570	Kentucky	MCCracken	1967-06-07		1			
MGG-180611-01	Kentucky	Muhlenberg	2018-06-11		1	8		*L.* aff. *polychromatus*
USNM 177548	Kentucky	Muhlenberg	1980-03-17	1		1	2	
USNM 85761	Kentucky	Muhlenberg	1941-05-13			1		
RFT-17-042	Kentucky	Union	2017-08-01		3			
RFT-17-043	Kentucky	Union	2017-08-01			2		
RFT-17-044	Kentucky	Union	2017-08-01		1	5		
MGG-170808-051	Tennesse	Carroll	2017-08-08		2			*L. ludovicianus*
USNM 260062	Tennesse	Henry	1989-08-06		1			
				18	37	69	19	
						Total:	143	

TABLE 2. Data on specimens used in our analyses including specimen code, species/clade, field and/or catalogue number, species/clade, State/Province and County of collection, and Genbank accession numbers for 12S, 16S and partial COI. Abbreviations: MGG, Mael G. Glon; USNM, Smithsonian National Museum of Natural History. Specific locality information has been retracted due to poaching concerns but is available from the primary author.

| Specimen code	Field #	Catalogue #	Species/clade	Country	State/Province	County	Genbank 12S	Genbank 16S	Genbank COI
MGG427	MGG-180316-01	USNM 1498707	*Lacunicambarus diogenes*	USA	Washington, D.C.	2nd Ward	MH878689	MH878721	MH882989
MGG429	MGG-180316-01	USNM 1498708	*Lacunicambarus diogenes*	USA	Washington, D.C.	2nd Ward	MH878690	MH878722	MH882990
MGG435	MGG-180515-01		*Lacunicambarus polychromatus*	Canada	Ontario	Essex	MH878691	MH878723	MH882991
MGG438	MGG-180611-01		*Lacunicambarus polychromatus*	USA	Kentucky	Muhlenberg	MH878692	MH878724	MH882992
MGG440	MGG-180611-01		*Lacunicambarus polychromatus*	USA	Kentucky	Muhlenberg	MH878693	MH878725	MH882993
MGG443	MGG-180612-01		*Lacunicambarus chimera*	USA	Kentucky	Hopkinds	MH878694	MH878726	MH882994
MGG446	MGG-180612-02		*Lacunicambarus polychromatus*	USA	Kentucky	Crittenden	MH878695	MH878727	MH882995
MGG450	MGG-180612-03		*Lacunicambarus chimera*	USA	Kentucky	Livingston	MH878696	MH878728	MH882996
MGG453	MGG-180612-04		*Lacunicambarus chimera*	USA	Kentucky	Graves	MH878697	MH878729	MH882997
MGG461	MGG-180613-01		*Lacunicambarus aff. diogenes*	USA	Missouri	Stoddard	MH878698	MH878730	MH882998
MGG467	MGG-180613-03		*Lacunicambarus chimera*	USA	Illinois	Pulaski	MH878699	MH878731	MH882999
MGG469	MGG-180613-05		*Lacunicambarus polychromatus*	USA	Illinois	Massac	MH878700	MH878732	MH883000
MGG472	MGG-180613-05		*Lacunicambarus chimera*	USA	Illinois	Massac	MH878701	MH878733	MH883001
MGG474	MGG-180614-01		*Creaserinus hortoni*	USA	Illinois	Massac	MH878702	MH878734	MH883002
MGG476	MGG-180614-01		*Lacunicambarus polychromatus*	USA	Illinois	Massac	MH878703	MH878735	MH883003
MGG479	MGG-180614-01		*Lacunicambarus chimera*	USA	Illinois	Massac	MH878704	MH878736	MH883004
MGG482	MGG-180614-01		*Lacunicambarus chimera*	USA	Illinois	Massac	MH878705	MH878737	MH883005
MGG484	MGG-180614-02		*Lacunicambarus aff. diogenes*	USA	Illinois	Pope	MH878706	MH878738	MH883006
MGG485	MGG-180614-02		*Lacunicambarus aff. diogenes*	USA	Illinois	Pope	MH878707	MH878739	MH883007
MGG487	MGG-180614-02		*Lacunicambarus polychromatus*	USA	Illinois	Pope	MH878708	MH878740	MH883008
MGG488	MGG-180614-03		*Lacunicambarus aff. diogenes*	USA	Illinois	Saline	MH878709	MH878741	MH883009
MGG489	MGG-180614-05		*Lacunicambarus polychromatus*	USA	Indiana	Posey	MH878710	MH878742	MH883010
MGG492	MGG-180614-06		*Lacunicambarus chimera*	USA	Illinois	White	MH878711	MH878743	MH883011
MGG493	MGG-180614-06		*Lacunicambarus chimera*	USA	Illinois	White	MH878712	MH878744	MH883012
MGG499	MGG-180615-01		*Lacunicambarus aff. diogenes*	USA	Illinois	Fayette	MH878713	MH878745	MH883013
MGG502	MGG-180615-01		*Lacunicambarus polychromatus*	USA	Illinois	Fayette	MH878714	MH878746	MH883014
MGG504	MGG-180615-02		*Lacunicambarus aff. diogenes*	USA	Illinois	Fayette	MH878715	MH878747	MH883015
MGG505	MGG-180615-02		*Lacunicambarus aff. diogenes*	USA	Illinois	Fayette	MH878716	MH878748	MH883016
MGG506	MGG-180615-02		*Lacunicambarus polychromatus*	USA	Illinois	Fayette	MH878717	MH878749	MH883017
MGG507	MGG-180615-03		*Lacunicambarus polychromatus*	USA	Illinois	Champaign	MH878718	MH878750	MH883018
MGG508	MGG-180615-03		*Lacunicambarus aff. diogenes*	USA	Illinois	Champaign	MH878719	MH878751	MH883019
MGG509	MGG-180615-03		*Lacunicambarus aff. diogenes*	USA	Illinois	Champaign	MH878720	MH878752	MH883020
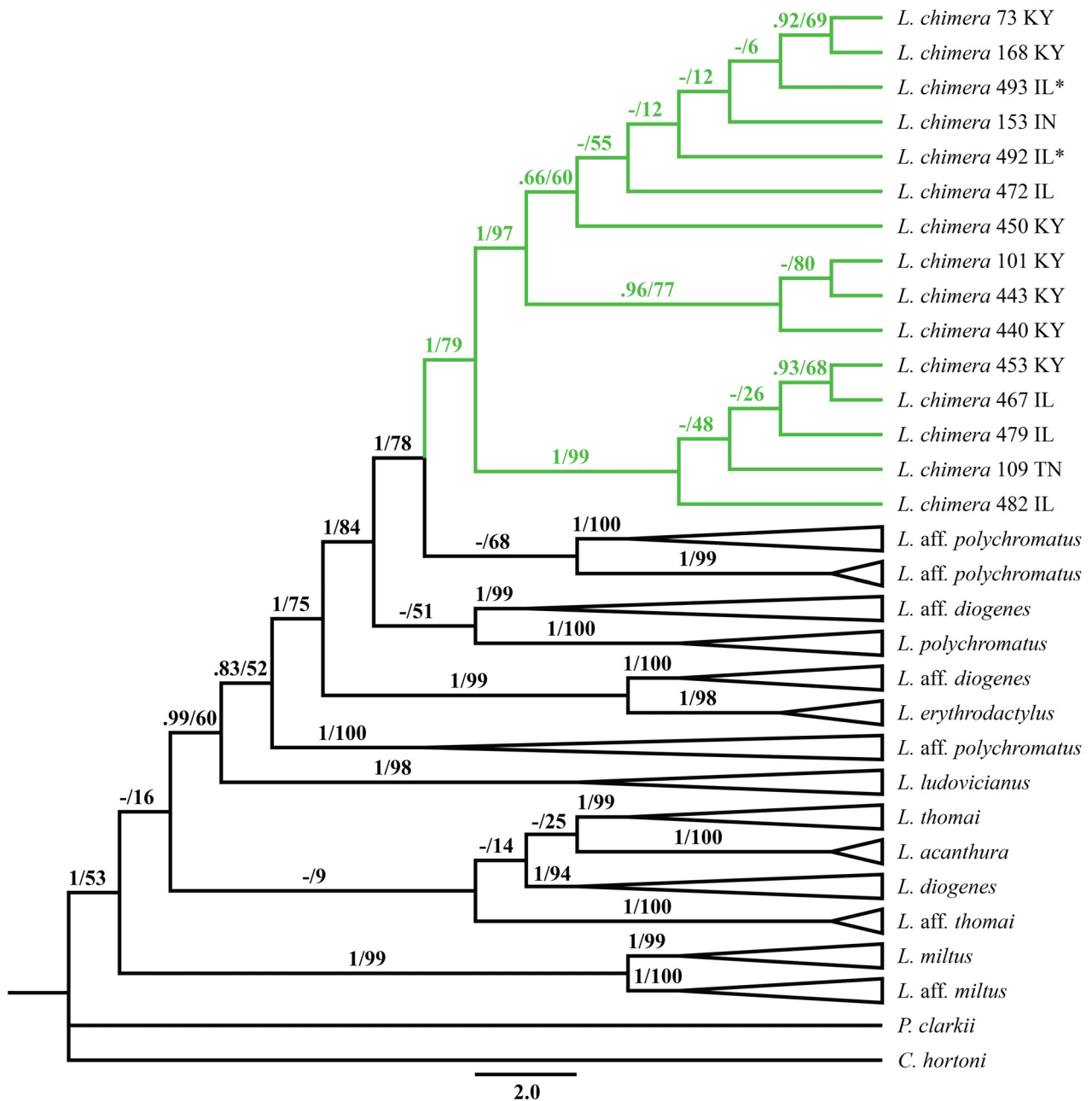
FIGURE 1. Phylogram showing maximum likelihood tree of *Lacunicambarus* estimated from three mitochondrial loci (partial 12S, partial 16S, and partial CO1). Bayesian posterior probability and maximum likelihood bootstrap support values are given in that order. Dashes indicate lack of nodal support. The *Lacunicambarus chimera* clade is highlighted in green with asterisks denoting specimens from the type locality. Numbers at tips correspond with specimen codes in Table 2, and abbreviations are States of collection (IL, Illinois; IN, Indiana; KY, Kentucky; TN, Tennessee). Other clades at the species level are collapsed into triangles to improve readability.

For Form II males, four measurements were significantly different between species following the Bonferroni correction (Table 3): acumen length/width, central projection length/gonopod length, mesial process length/ gonopod length, and number of spines on the ventrolateral margin of the merus. However, this combination of parameters did not provide sufficient resolution for the NMDS to converge, so we also included the number of tubercles on the mesial margin of the dactyl in this NMDS. The number of tubercles on the mesial margin of the dactyl was significantly different between species in our three other partitions and was clearly different and taxonomically informative between Form II males of both species (*L. chimera* mean ± standard deviation [sd] =

21.25 ± 3.53, *L. diogenes* mean ± sd = 16.11 ± 3.76; p = 0.004) despite not being considered significant due to the highly conservative nature of the Bonferroni correction. After adding the number of tubercles on the mesial margin of the dactyl to the dataset, our NMDS converged on a two-dimensional solution with an acceptable stress level (non-metric fit R^2 = 0.99; linear fit R^2 = 0.97; stress = 0.07). *Lacunicambarus chimera* and *L. diogenes* form two clusters of points with minimal overlap on our NMDS plot for this partition (Figure 4).

For females, eight measurements were significantly different between species following the Bonferroni correction (Table 3): antennal scale length/width, palm length/propodus length, palm depth/propodus length, dactyl length/propodus length, annulus ventralis length/width, number of anteroventral branchiostegal tubercles, number of spines on the ventrolateral margin of the merus, and number of tubercles on the mesial margin of dactyl. Our NMDS converged on a two-dimensional solution with an acceptable stress level (non-metric fit R^2 = 0.99; linear fit R^2 = 0.96; stress = 0.104). *Lacunicambarus chimera* and *L. diogenes* form two clusters of points with a small amount of overlap on our NMDS plot for this partition (Figure 5).
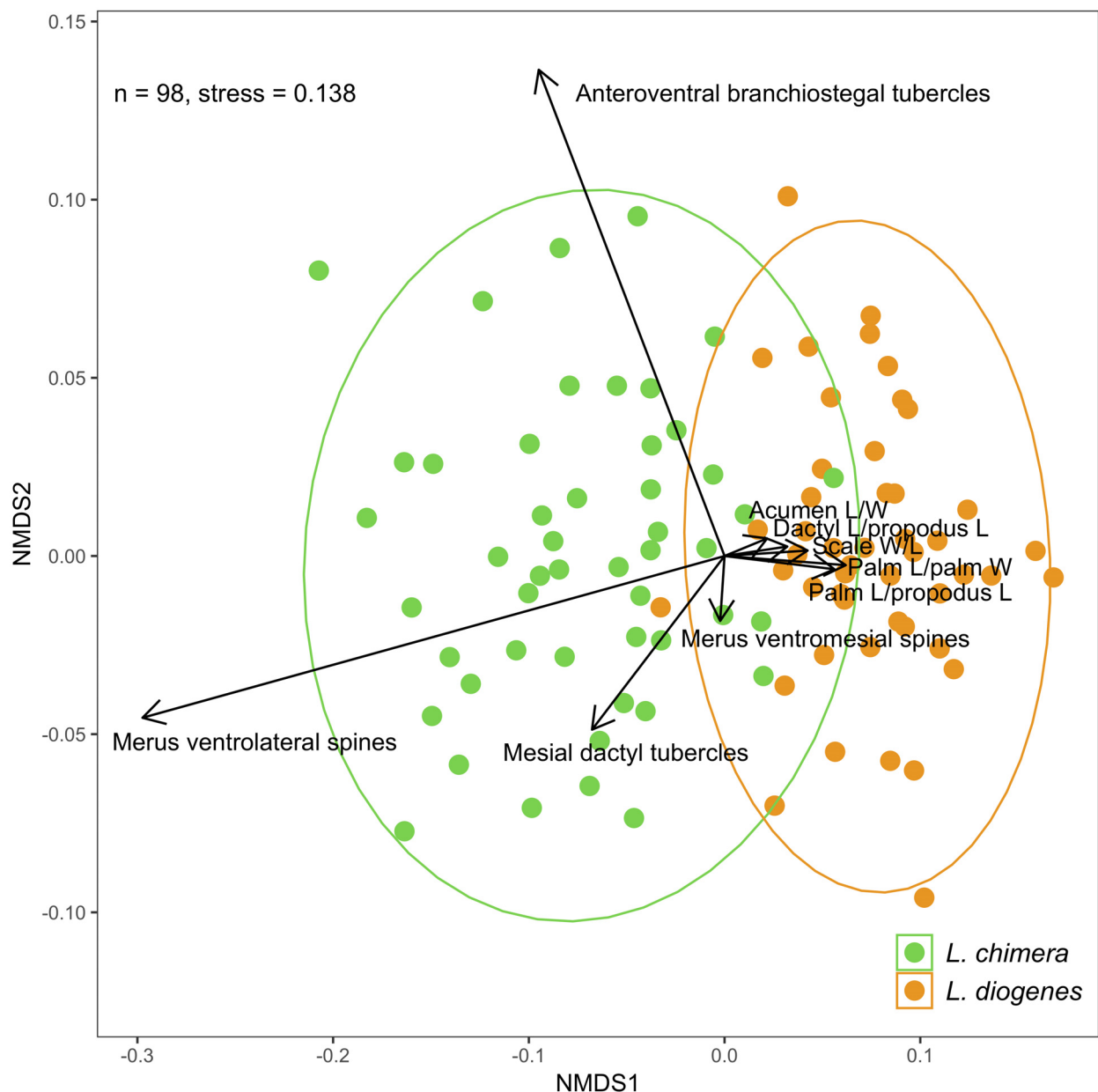

FIGURE 2. Non-metric multidimensional scaling (NMDS) plot of complete data set (n = 98) showing differences in morphological and meristic characters between *Lacunicambarus chimera* and *L. diogenes*. Vectors represent strength and direction of correlation of each character relative to the NMDS axes. This NMDS converged on a two-dimensional solution with an acceptable stress level (non-metric fit R^2 = 0.91; linear fit R^2 = 0.92; stress = 0.133). Abbreviations: L, length; W, width.

TABLE 3. Statistical data grouped by data partition (all specimens, Form I males, Form II males, and females) including mean and standard deviation of each ratio or measurement for *Lacunicambarus chimera* sp. nov. and *L. diogenes*, test statistic and p-values of pairwise comparison between species (W for Wilcoxon Rank-Sum Test, t for Welch's t-test), and statistical significance after Bonferroni correction.

Data Partition	Ratio/measurement	Species	Mean	Standard deviation	Test statistic	p-value	Significant at Bonferroni corrected alpha (p = 0.05/ # comparisons)?
Full data set (n = 49 of each species)	Carapace width/carapace length	*L. chimera*	0.48	0.03	W = 1200	0.474	no
		L. diogenes	0.48	0.02			
	Carapace depth/carapace length	*L. chimera*	0.49	0.02	t = -1.88	0.064	no
		L. diogenes	0.50	0.02			
	Areola length/carapace length	*L. chimera*	0.42	0.01	W = 769	0.011	no
		L. diogenes	0.42	0.01			
	Cephalon width/cephalon length	*L. chimera*	0.67	0.02	t = -2.63	0.01	no
		L. diogenes	0.68	0.03			
	Postorbital ridge width/cephalon width	*L. chimera*	0.49	0.03	t = -1.05	0.296	no
		L. diogenes	0.50	0.03			
	Rostrum width at eyes/rostrum length	*L. chimera*	0.75	0.05	t = -0.18	0.857	no
		L. diogenes	0.76	0.07			
	Rostrum length/cephalon length	*L. chimera*	0.27	0.02	t = 3.07	0.003	no
		L. diogenes	0.26	0.02			
	Acumen length/acumen width	*L. chimera*	0.62	0.11	W = 1706	<0.0001	yes
		L. diogenes	0.55	0.12			
	Antennal scale length/width	*L. chimera*	0.36	0.03	t = 5.04	<0.0001	yes
		L. diogenes	0.34	0.03			
	Palm length/propodus length	*L. chimera*	0.31	0.02	t = -5.00	<0.0001	yes
		L. diogenes	0.32	0.02			
	Palm length/palm width	*L. chimera*	0.66	0.04	t = -3.4	0.001	yes
		L. diogenes	0.68	0.04			
	Palm depth/propodus length	*L. chimera*	0.28	0.02	W = 749	0.007	no
		L. diogenes	0.29	0.03			
	Dactyl length/propodus length	*L. chimera*	0.65	0.02	t = 5.67	<0.0001	yes
		L. diogenes	0.63	0.02			
	Cervical tubercles	*L. chimera*	5.74	2.18	W = 1330	0.078	no
		L. diogenes	5.19	1.77			
	Anteroventral branchiostegal tubercles	*L. chimera*	17.81	8.23	W = 1796	<0.0001	yes
		L. diogenes	12.32	4.53			
	Merus ventromesial spines	*L. chimera*	11.30	2.31	t = 8.67	<0.0001	yes
		L. diogenes	9.85	1.81			
	Merus ventrolateral spines	*L. chimera*	4.89	2.49	W = 2105	<0.0001	yes
		L. diogenes	1.83	1.06			
	Mesial dactyl tubercles	*L. chimera*	21.74	5.22	W = 1700	<0.0001	yes
		L. diogenes	15.49	5.22			

TABLE 3. (Continued)
Form 1 males (n = 10, *L. chimera*; n = 17, *L. diogenes*)

Carapace width/carapace length	*L. chimera*	0.50	0.02	W = 130	0.02347	no
	L. diogenes	0.48	0.02			
Carapace depth/carapace length	*L. chimera*	0.50	0.02	t = 0.39	0.7	no
	L. diogenes	0.50	0.02			
Areola length/carapace length	*L. chimera*	0.43	0.01	t = 2.01	0.059	no
	L. diogenes	0.42	0.01			
Cephalon width/cephalon length	*L. chimera*	0.69	0.02	t = 1.27	0.218	no
	L. diogenes	0.68	0.03			
Postorbital ridge width/cephalon width	*L. chimera*	0.49	0.02	t = -2.63	0.015	no
	L. diogenes	0.50	0.02			
Rostrum width at eyes/rostrum length	*L. chimera*	0.78	0.04	t = 1.51	0.134	no
	L. diogenes	0.75	0.06			
Rostrum length/cephalon length	*L. chimera*	0.26	0.02	t = -3.02	0.765	no
	L. diogenes	0.26	0.02			
Acumen length/acumen width	*L. chimera*	0.55	0.13	t = 0.38	0.706	no
	L. diogenes	0.54	0.09			
Antennal scale length/width	*L. chimera*	0.36	0.06	t = 2.29	0.038	no
	L. diogenes	0.33	0.03			
Palm length/propodus length	*L. chimera*	0.31	0.04	t = -1.46	0.173	no
	L. diogenes	0.32	0.01			
Palm length/palm width	*L. chimera*	0.67	0.07	t = -0.17	0.868	no
	L. diogenes	0.67	0.04			
Palm depth/propodus length	*L. chimera*	0.27	0.03	t = -2.52	0.0198	no
	L. diogenes	0.29	0.02			
Dactyl length/propodus length	*L. chimera*	0.64	0.03	t = 1.18	0.256	no
	L. diogenes	0.64	0.02			
Gonopod umbo width/gonopod length	*L. chimera*	0.28	0.02	t = -4.51	<0.001	yes
	L. diogenes	0.30	0.02			
Central projection length/gonopod length	*L. chimera*	0.22	0.01	W = 0	<0.0001	yes
	L. diogenes	0.29	0.01			
Mesial process length/gonopod length	*L. chimera*	0.26	0.02	t = -9.12	<0.0001	yes
	L. diogenes	0.31	0.02			
Cervical tubercles	*L. chimera*	5.00	2.57	t = 0	1	no
	L. diogenes	5.00	1.41			
Anteroventral branchiostegal tubercles	*L. chimera*	20.20	13.79	W = 148	0.002	yes
	L. diogenes	10.82	3.49			
Merus ventromesial spines	*L. chimera*	11.40	2.08	W = 170	<0.0001	yes
	L. diogenes	9.24	1.38			
Merus ventrolateral spines	*L. chimera*	5.80	2.42	t = 4.51	<0.001	yes
	L. diogenes	1.65	0.76			
Mesial dactyl tubercles	*L. chimera*	23.10	5.77	t = 6.99	<0.0001	yes
	L. diogenes	14.29	3.08			

TABLE 3. (Continued)

Form II males (n = 16, *L. chimera*; n = 9, *L. diogenes*)

Character	Species					
Carapace width/carapace length	*L. chimera*	0.47	0.03	W = 65	0.718	no
	L. diogenes	0.48	0.02			
Carapace depth/carapace length	*L. chimera*	0.49	0.01	t = -0.95	0.365	no
	L. diogenes	0.49	0.04			
Areola length/carapace length	*L. chimera*	0.41	0.01	t = -1.22	0.242	no
	L. diogenes	0.42	0.02			
Cephalon width/cephalon length	*L. chimera*	0.67	0.02	W = 59	0.487	no
	L. diogenes	0.68	0.03			
Postorbital ridge width/cephalon width	*L. chimera*	0.51	0.02	t = 0.71	0.488	no
	L. diogenes	0.50	0.04			
Rostrum width at eyes/rostrum length	*L. chimera*	0.76	0.04	t = -0.72	0.485	no
	L. diogenes	0.77	0.07			
Rostrum length/cephalon length	*L. chimera*	0.27	0.01	t = 2.18	0.043	no
	L. diogenes	0.26	0.02			
Acumen length/acumen width	*L. chimera*	0.65	0.08	t = 4.4	<0.001	yes
	L. diogenes	0.55	0.08			
Antennal scale length/width	*L. chimera*	0.35	0.03	t = 1.403	0.179	no
	L. diogenes	0.34	0.04			
Palm length/propodus length	*L. chimera*	0.31	0.02	t = -1.78	0.091	no
	L. diogenes	0.32	0.02			
Palm length/palm width	*L. chimera*	0.66	0.02	t = -2.71	0.018	no
	L. diogenes	0.69	0.04			
Palm depth/propodus length	*L. chimera*	0.29	0.02	t = -0.47	0.643	no
	L. diogenes	0.29	0.03			
Dactyl length/propodus length	*L. chimera*	0.65	0.02	t = 3.04	0.007	no
	L. diogenes	0.63	0.03			
Gonopod umbo width/gonopod length	*L. chimera*	0.28	0.01	t = -2.10	0.064	no
	L. diogenes	0.30	0.05			
Central projection length/gonopod length	*L. chimera*	0.27	0.02	W = 3	<0.0001	yes
	L. diogenes	0.32	0.03			
Mesial process length/gonopod length	*L. chimera*	0.30	0.02	t = 6.46	<0.0001	yes
	L. diogenes	0.35	0.04			
Cervical tubercles	*L. chimera*	5.75	1.48	W = 84.5	0.482	no
	L. diogenes	5.22	2.61			
Anteroventral branchiostegal tubercles	*L. chimera*	14.94	4.37	W = 101	0.104	no
	L. diogenes	12.44	5.72			
Merus ventromesial spines	*L. chimera*	11.25	1.68	t = 2.37	0.033	no
	L. diogenes	9.67	2.89			
Merus ventrolateral spines	*L. chimera*	4.69	2.36	W = 131	<0.001	yes
	L. diogenes	1.89	1.00			
Mesial dactyl tubercles	*L. chimera*	21.25	4.41	t = 3.35	0.004	no
	L. diogenes	16.11	6.26			

TABLE 3. (Continued)

Females (n = 23 of each species)

| Character	Species	Mean	SD	Statistic	p	Significant
Carapace width/carapace length	L. chimera	0.49	0.02	t = 0.58	0.565	no
	L. diogenes	0.48	0.02			
Carapace depth/carapace length	L. chimera	0.49	0.02	t = -1.40	0.168	no
	L. diogenes	0.50	0.02			
Areola length/carapace length	L. chimera	0.41	0.01	t = -3.14	0.003	no
	L. diogenes	0.42	0.01			
Cephalon width/cephalon length	L. chimera	0.67	0.02	t = -2.72	0.009	no
	L. diogenes	0.69	0.03			
Postorbital ridge width/cephalon width	L. chimera	0.49	0.03	t = -0.979	0.333	no
	L. diogenes	0.50	0.03			
Rostrum width at eyes/rostrum length	L. chimera	0.75	0.06	t = -0.39	0.698	no
	L. diogenes	0.75	0.08			
Rostrum length/cephalon length	L. chimera	0.27	0.01	t = 1.55	0.129	no
	L. diogenes	0.26	0.02			
Acumen length/acumen width	L. chimera	0.62	0.09	W = 392	0.005	no
	L. diogenes	0.57	0.14			
Antennal scale length/width	L. chimera	0.36	0.03	t = 4.56	<0.0001	yes
	L. diogenes	0.34	0.03			
Palm length/propodus length	L. chimera	0.31	0.02	t = -3.99	<0.001	yes
	L. diogenes	0.33	0.02			
Palm length/palm width	L. chimera	0.65	0.04	t = -2.51	0.016	no
	L. diogenes	0.67	0.05			
Palm depth/propodus length	L. chimera	0.28	0.02	t = -3.73	<0.001	yes
	L. diogenes	0.30	0.02			
Dactyl length/propodus length	L. chimera	0.65	0.02	t = 4.42	<0.0001	yes
	L. diogenes	0.62	0.02			
Annulus ventralis length/width	L. chimera	0.76	0.13	t = -4.38	<0.0001	yes
	L. diogenes	0.88	0.13			
Cervical tubercles	L. chimera	6.13	2.31	W = 349	0.056	no
	L. diogenes	5.26	1.77			
Anteroventral branchiostegal tubercles	L. chimera	18.74	6.61	W = 345	<0.001	yes
	L. diogenes	13.39	4.38			
Merus ventromesial spines	L. chimera	11.30	2.64	W = 365.5	0.023	no
	L. diogenes	10.30	1.38			
Merus ventrolateral spines	L. chimera	4.91	2.59	W = 506	<0.0001	yes
	L. diogenes	1.87	1.23			
Mesial dactyl tubercles	L. chimera	21.30	5.11	t = 4.7382	<0.0001	yes
	L. diogenes	16.26	5.10			
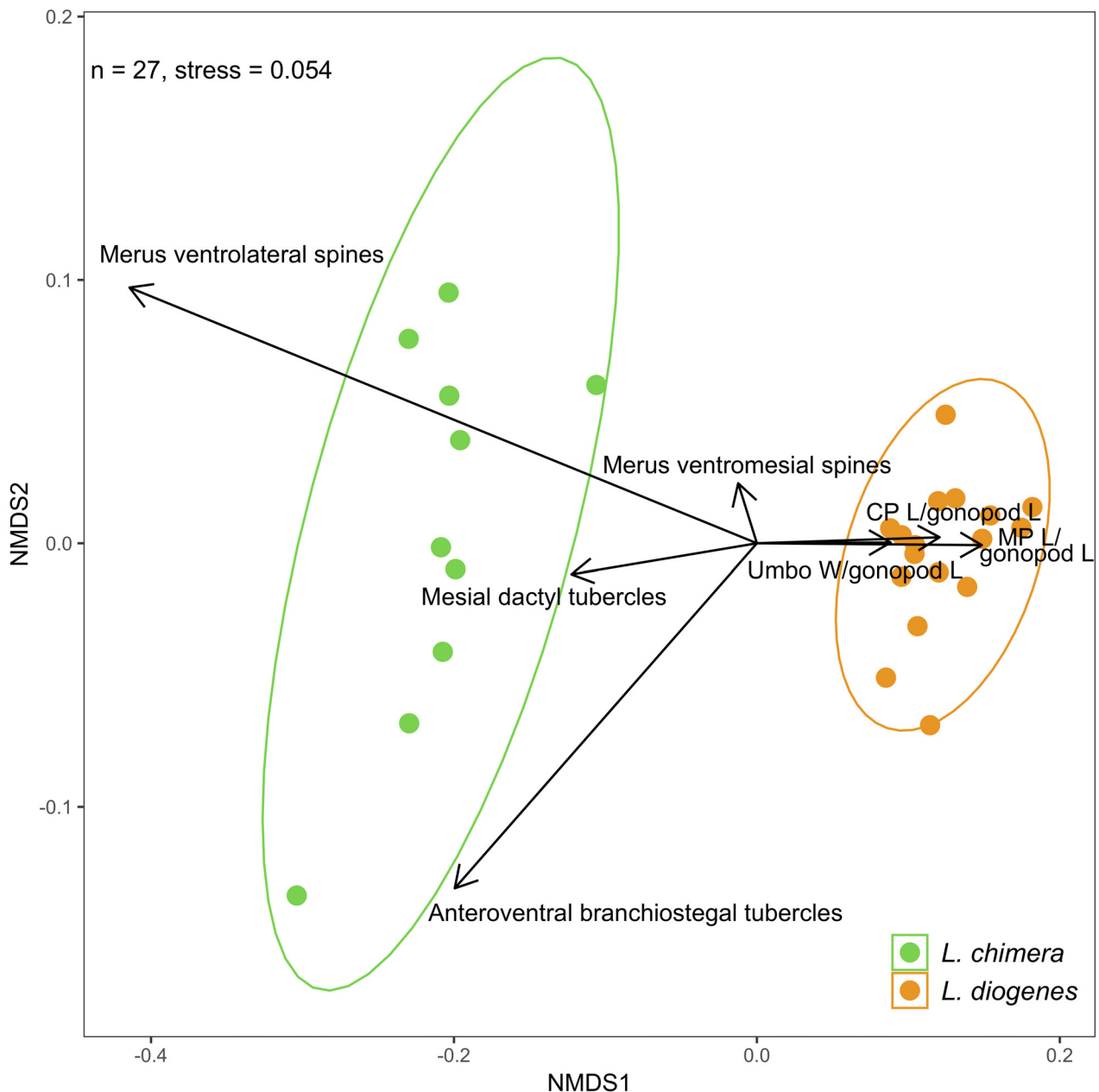
FIGURE 3. Non-metric multidimensional scaling (NMDS) plot for Form I males (n = 27) showing differences in morphological and meristic characters between *Lacunicambarus chimera* and *L. diogenes*. Vectors represent strength and direction of correlation of each character relative to the NMDS axes. This NMDS converged on a two-dimensional solution with an acceptable stress level (non-metric fit $R^2 = 0.99$; linear fit $R^2 = 0.99$; stress = 0.054). Abbreviations: L, length; W, width; CP, central projection; MP mesial process.

Taxonomy

Family Cambaridae Hobbs 1942

Genus *Lacunicambarus* (Hobbs 1969)

Lacunicambarus chimera Glon & Thoma sp. nov.
(Figures 6, 7)

Cambarus obesus Forbes 1876:6 [in part].

Cambarus diogenes Hay 1895:478 [in part]. Ortmann 1905:123 [in part]. Rhoades 1944:111 [in part]. Eberly 1954:283 [in part]. Brown 1955:62 [in part]. Marlow 1960:229 [in part]. Page 1985:433 [in part]. Page & Mottesi 1995:23 [in part]. Taylor *et al.* 1996:29 [in part]. Simon 2001:104 [in part]. Taylor *et al.* 2007:382 [in part]. Taylor & Schuster 2004:80 [in part]. Taylor Schuster & Wylie 2015:66 [in part].

Cambarus diogenes diogenes Marlow 1960:233 [in part].

Cambarus (*Lacunicambarus*) *diogenes diogenes* Hobbs 1969:110 [in part]; 1974:20 [in part]. Bouchard 1972:56 [in part]; 1974:595 [in part].

Cambarus (*Lacunicambarus*) *diogenes* Hobbs 1989: 24 [in part]. Thoma *et al. 2005*:334 [in part]. Thoma & Armitage 2008:iii [in part].

Cambarus cf. *diogenes* Glon 2017:55.

Lacunicambarus aff. *diogenes* Glon *et al.* 2018:604 [in part].

Diagnosis. Eyes pigmented, not reduced. Rostrum curved downwards in lateral view, margins converging, slightly thickened, without marginal spines or tubercles, lacking median carina, shallowly excavated. Acumen distinctly delimited basally by 45° angles. Cephalothorax cylindrical, with 3–10 (mean ± sd: 6 ± 1) small tubercles lining posterior margin of cervical groove. Anteroventral branchiostegal tubercles small, numbering 8–29 (mean ± sd: 18 ± 4). Suborbital angle acute. Postorbital ridges developed, lacking anterior spine or tubercle. Areola obliterated, constituting, in adults, 38–45% (mean ± sd: 42 ± 0 %) of entire length of cephalothorax. Antennal scale 2.41 to 3.35 (mean ± sd: 2.80 ± 0.18) times as long as wide, broadest distal to midlength, terminating in small spine, mesial margin forming straight edge. Dorsomesial margin of palm of chelae with 3 rows of tubercles, mesial-most row normally consisting of 6–10 (mean ± sd: 7 ± 1) probolos tubercles, running parallel to second row with 4–9 (mean ± sd: 6 ± 1) probolos tubercles, third row running diagonally from mesial base of palm to lateral dactyl articulation in the form of 5–8 (mean ± sd: 7 ± 1) subprobolos tubercles located in shallow dimples. No tufts of elongated setae at mesial base of fixed finger. Opposable margin of dactyl weakly concave at base. Ratio of dactyl length to palm length 1.78–2.49 (mean ± sd: 2.10 ± 0.16). Dorsomedian longitudinal ridges of dactyl and fixed finger of propodus weakly developed. Dorsolateral impression at base of propodus moderate. Ventral surface of chelae with 0–5 (mean ± sd: 2 ± 1) subpalmar tubercles. Mesial margin of dactyl with 12–33 (mean ± sd: 22 ± 4) prominent tubercles. Ventral surface of carpus with single spine on mesial articular rim, mesial margin with 4–10 (mean ± sd: 7 ± 1) spines of varying sizes. Merus spines numbering 2–9 (mean: 5 ± 2) on ventrolateral margin and 7–16 (mean ± sd: 11 ± 2) on ventromesial margin. Mesial ramus of uropod with distomedian spine not reaching caudal margin. Gonopods of Form I males contiguous at base, with moderately pronounced umbo near midlength of caudal surface; terminal elements consisting of 1) short, tapering, distally truncate central projection lacking subapical notch, shorter than mesial process, directed caudally at approximately 90°, reaching past margin of umbo, 2) mesial process with conical base tipped with protruding finger, directed caudally at approximately 90° and overreaching umbo by noticeable amount and 3) inconspicuous caudal knob sometimes present at caudolateral base of central projection. Hooks on ischium of third pereiopods only. Female with annulus ventralis subquadrangular or kite-shaped, approximately as long as wide, rather deeply embedded in sternum, flexible, with posterior half sclerotized and anterior half mildly pliable.

Holotypic male, Form I (OSUMC 10650; Figures 6, 7A–D, G–J, L–M). Body subovate (Figure 7J), cephalothorax depth 95% of width (Table 4). Abdomen narrower than cephalothorax (23.82 and 31.20 mm, respectively; Figure 6); maximum width of cephalothorax greater than depth at caudodorsal margin of cervical groove (31.20 and 29.73 mm, respectively). Areola obliterated; length 45% of total length of cephalothorax (Figure 7J). Rostrum curved downwards in lateral view from base to distal end, margins slightly thickened; acumen distinctly delimited basally by 45° angles, anterior tip upturned and not reaching ultimate podomere of antennular peduncle; upper surface of rostrum shallowly concave with minute punctations forming single row bordering margin. Subrostral ridge weak but evident in lateral aspect along entire length of rostrum. Postorbital ridges developed, grooved dorsolaterally, ending cephalically without spine or corneous tubercle. Suborbital angle acute; branchiostegal spine replaced by small spiniform tubercle. Posterior margin of cervical groove lined by 5 tubercles, single larger tubercle present in cervical groove. Branchiostegal region smooth. Anteroventral branchiostegal region with 14 small tubercles. Hepatic region with scattered small tubercles. Remainder of cephalothorax with slight punctations dorsal and laterally. Abdomen subequal in length to cephalothorax, 2.5 times as long as wide; pleura short, truncate, rounded caudoventrally. Cephalic section of telson with 2 spines in caudolateral corners, mesial spine moveable. Proximal segment of lateral ramus of uropod with 23 spines on distal margin, second most lateral spine distinctly longer than others; mesial ramus of uropod with prominent median rib ending distally as strong distomedian spine not reaching margin of ramus, laterodistal spine of ramus strong and curved mesially.

Cephalomedian lobe of epistome (Figure 7I) bell-shaped with uniform raised margins, lightly setate, ventral surface flat; main body of epistome with shallow fovea; epistomal zygoma mildly arched. Ventral surface of antennular peduncle's proximal podomere with small spine at midlength. Antennal peduncle without spines; antennal scale 2.66 times as long as wide (Figure 7L), broadest distal to midlength, mesial margin straight from basal area to broadest distal point; distal antennal spine reduced, not reaching distal margin of penultimate podomore of antennal peduncle. Lateral half of ischium of third maxilliped densely studded with long, flexible setae; distolateral angle acute, spiniform.
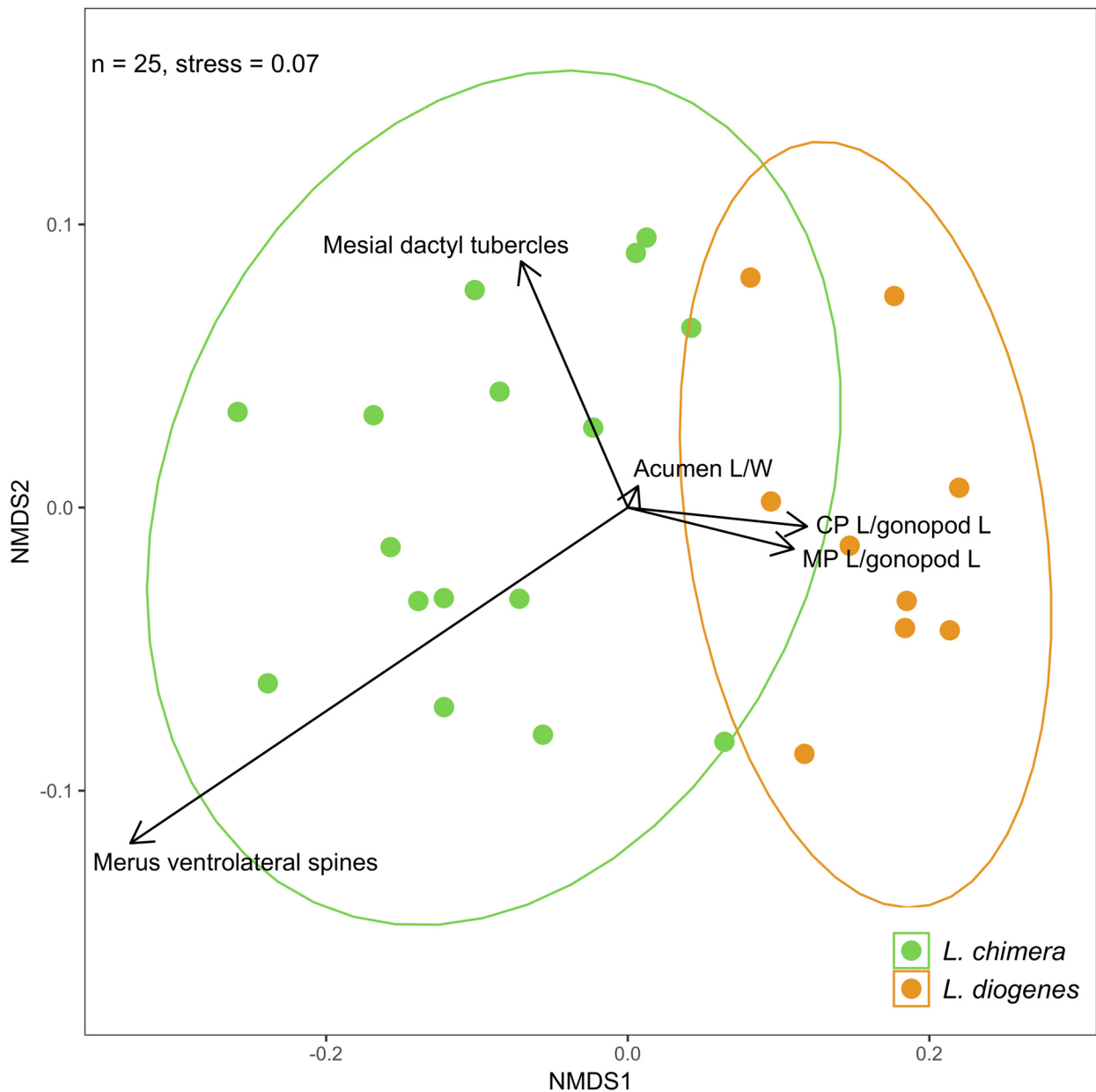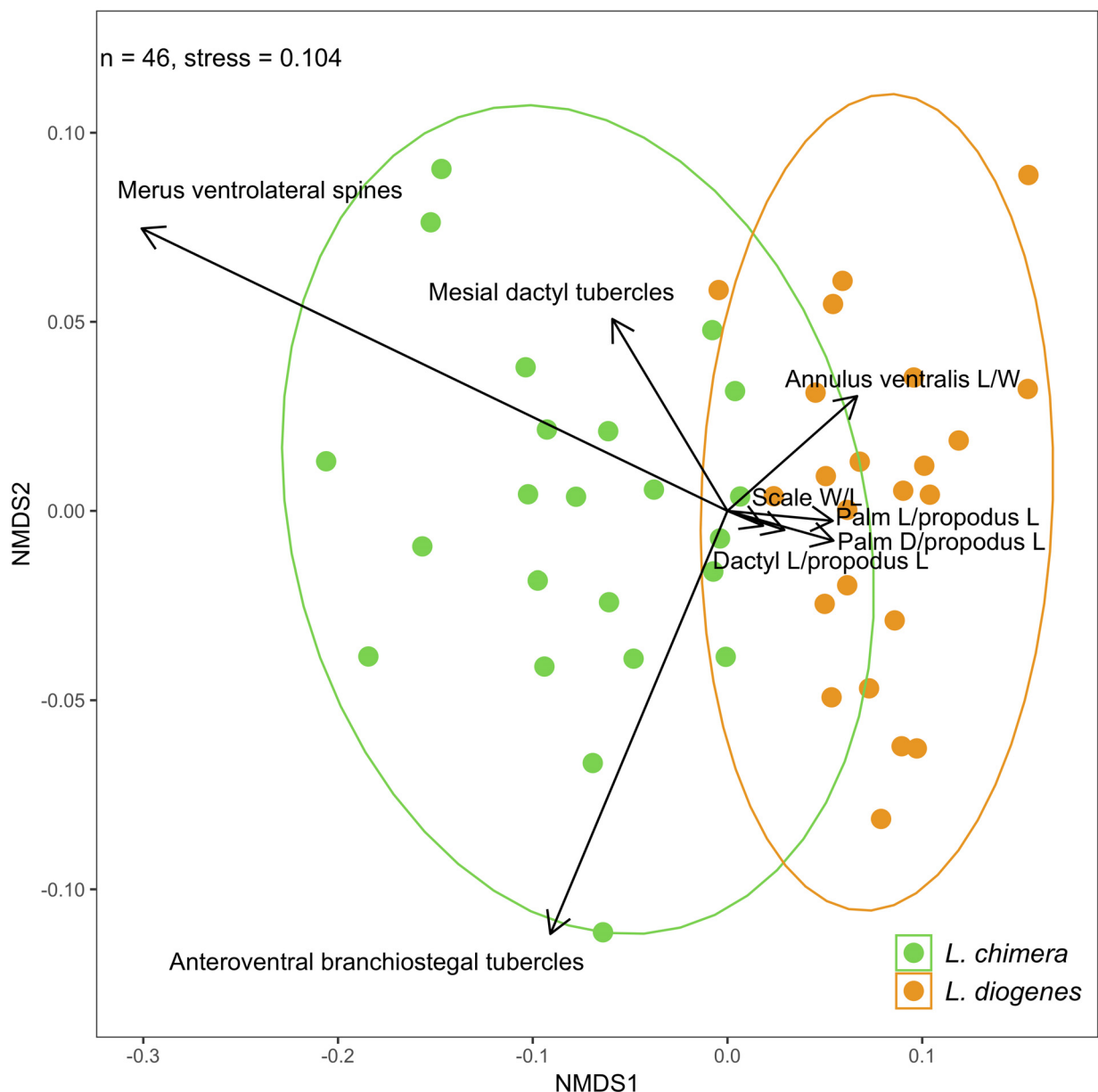

FIGURE 4. Non-metric multidimensional scaling (NMDS) plot for Form II males (n = 25) showing differences in morphological and meristic characters between *Lacunicambarus chimera* and *L. diogenes*. Vectors represent strength and direction of correlation of each character relative to the NMDS axes. This NMDS converged on a two-dimensional solution with an acceptable stress level (non-metric fit $R^2 = 0.99$; linear fit $R^2 = 0.97$; stress = 0.07). Abbreviations: L, length; W, width; CP, central projection; MP, mesial process.

Length of right chela (Figure 7M) 103% of cephalothorax length; chela width 44% of chela length; palm length 31% of chela length; dactyl length 2.11 times palm length. Dorsomesial margin of palm of chela with 3 rows of tubercles, mesial-most row composed of 8 tubercles running parallel to second row of 6 tubercles, third row running diagonally from mesial base of palm to lateral dactyl articulation comprised of 6 subprobolos tubercles

located in shallow dimples, 4 distal tubercles between second and third (diagonal) row, dorsal, proximal dorsolateral half smooth, most distolateral area punctate, punctations moderately defined in vicinity of dorsolateral base of propodus; lateral margin of propodus not costate; ventromesial surface with small punctations, 2 bulbous tubercles on propodactyl articular rim; 5 subpalmar tubercles, 3 located proximally to ventral dactyl articulation, 2 located laterally to ventral dactyl articulation. Both fingers of chela with weakly developed dorsomedian longitudinal ridges. Opposable margin of propodus with row of 8 tubercles, decreasing in size except for third from base which is greatly enlarged over adjacent tubercles, ultimate tubercle with corneous tip, larger than penultimate tubercle, positioned ventrally relative to adjacent tubercles; single row of minute denticles extending distally from fifth tubercle. Opposable margin of dactyl with row of 8 tubercles approximately equal in size except for fourth from base which is enlarged over adjacent tubercles; single row of minute denticles extending distally from sixth tubercle; mesial surface of dactyl studded with 25 tubercles basally, not forming distinct rows, giving way to punctations distally. Dorsolateral impression at base of propodus moderate.

FIGURE 5. Non-metric multidimensional scaling (NMDS) plot for females (n = 46) showing differences in morphological and meristic characters between *Lacunicambarus chimera* and *L. diogenes*. Vectors represent strength and direction of correlation of each character relative to the NMDS axes. This NMDS converged on a two-dimensional solution with an acceptable stress level (non-metric fit $R^2 = 0.99$; linear fit $R^2 = 0.96$; stress = 0.104). Abbreviations: L, length; W, width; D, depth.

Cheliped carpus with distinct dorsal furrow; dorsomesial surface with row of 8 tubercles; dorsolateral surface with 11 punctations; mesial surface with row of 4 small spines plus 1 large procurved spine near distal margin, 3 spiniform tubercles triangularly arranged and located ventral to spines; ventral surface with spine on distal articular rim. Merus with 2 pre-marginal spines dorsally, ventrolateral margin with row of 6 spines, ventromesial margin with row of 13 spines, increasing in size from base (Figure 7H). Basioischial segment of first pereiopod with 4 small tubercles on ventral margin. Ischium of third pereiopod with simple hook extending proximally over basioischial articulation, not opposed by tubercles on basis (Figure 7G). Coxa of fourth pereiopod with setiferous, vertically disposed caudomesial boss, ventral surface calcified; coxa of fifth pereiopod lacking boss, ventral surface membranous.

Gonopods contiguous at base, reaching past caudomesial boss of fourth pereiopod; central projection (Figure 7B–D) short, tapering, lacking subapical notch, directed caudally at approximately 90°, shorter than mesial process, just overreaching umbo; mesial process conical at base, then tipped with protruding finger, directed caudally at approximately 90°, overreaching umbo; caudal knob inconspicuous but present at caudolateral base of central projection.

Sinistral gonopod, sinistral antennal scale, and sinistral second pleopod of specimen separated from specimen and placed in glass vials inside specimen jar. Dextral antenna missing from specimen. Two gills were extracted from sinistral gill chamber of specimen and preserved in 100% ethanol for future DNA extractions; one is frozen in the OSUMC crustacean collection (MGG 528) and the other was deposited as a tissue sample in the USNM biorepository (USNM 1480291).

Allotypic female (OSUMC 10652; Figure 7K). The allotypic female differs from the holotype as follows: cephalothorax depth 106% of width (Table 4). Abdomen wider than cephalothorax (31.91 and 30.91 mm, respectively); maximum width of cephalothorax less than depth at caudodorsal margin of cervical groove (30.90 and 32.65 mm, respectively). Areola length 41% of total length of cephalothorax. Posterior margin of cervical groove lined by 8 tubercles, lacking single larger tubercle in cervical groove. Anteroventral branchiostegal region with 23 small tubercles. Abdomen greater in length than cephalothorax, 2.01 times as long as wide. Cephalomedian lobe of epistome bell-shaped. Antennal scale 2.57 times as long as wide.

FIGURE 6. Dorsal view of Form I holotypic male of *Lacunicambarus chimera* (OSUMC 10650). Photo by Guenter Schuster.
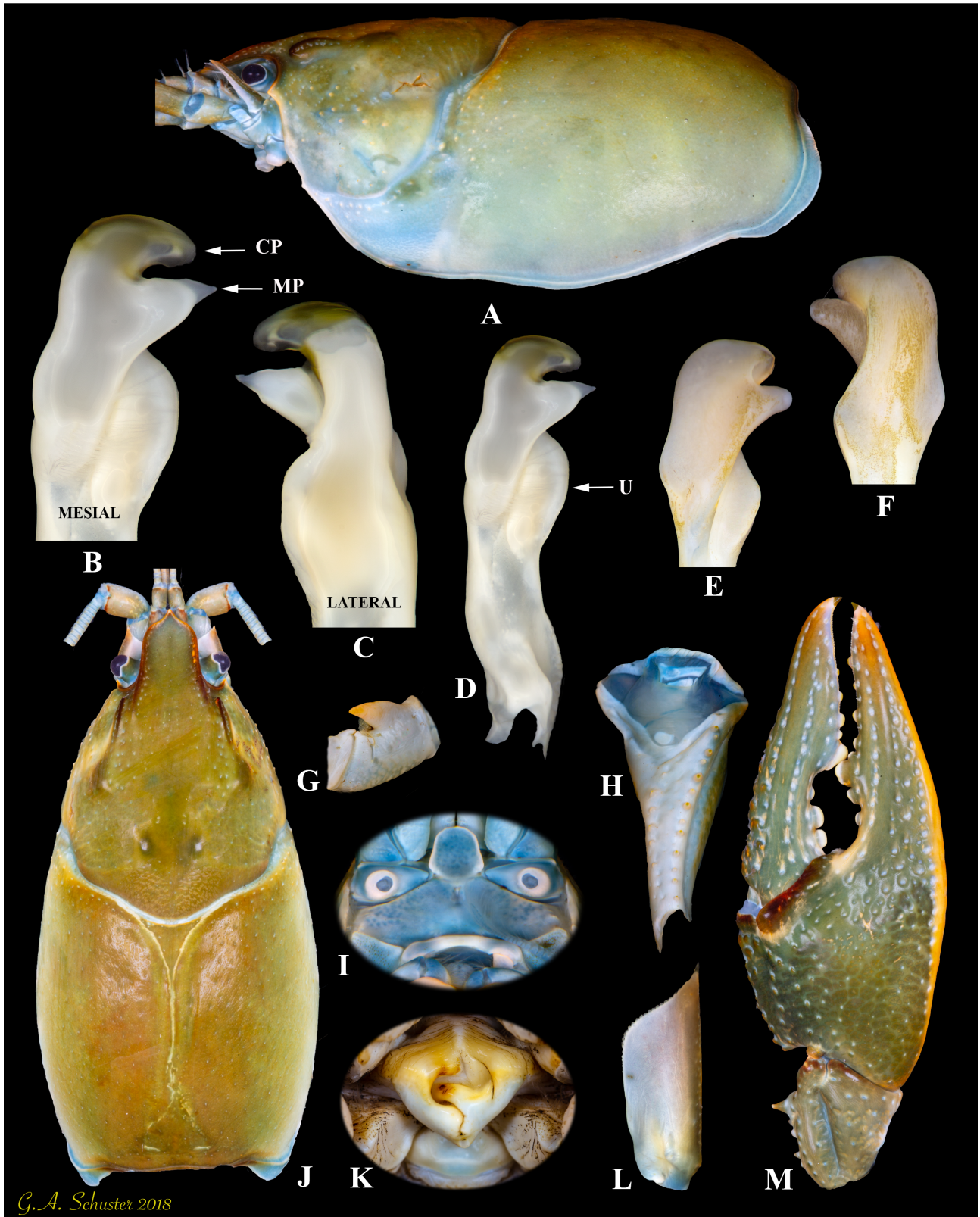
FIGURE 7. Form I holotypic male of *Lacunicambarus chimera*. (OSUMC 10650) (A–D, G–J, L–M); Form II morphotype (OSUMC 10651) (E, F); Allotype (OSUMC 10652) (K). Lateral view of cephalothorax (A); mesial and lateral views of Form I gonopod (B–D); mesial and lateral views of Form II gonopod (E, F); ischial hook (G); ventral view of merus (H); epistome (I); dorsal view of cephalothorax (J); annulus ventralis (K); dorsal view of antennal scale (L); dorsal view of chela (M). Photos by Guenter Schuster. Abbreviations: CP, central projection; MP, mesial process; U, umbo.

FIGURE 8. Dorsal view of juvenile *Lacunicambarus chimera* specimen from Pike County, Indiana (MGG-170812-03). Photo by Mael Glon.
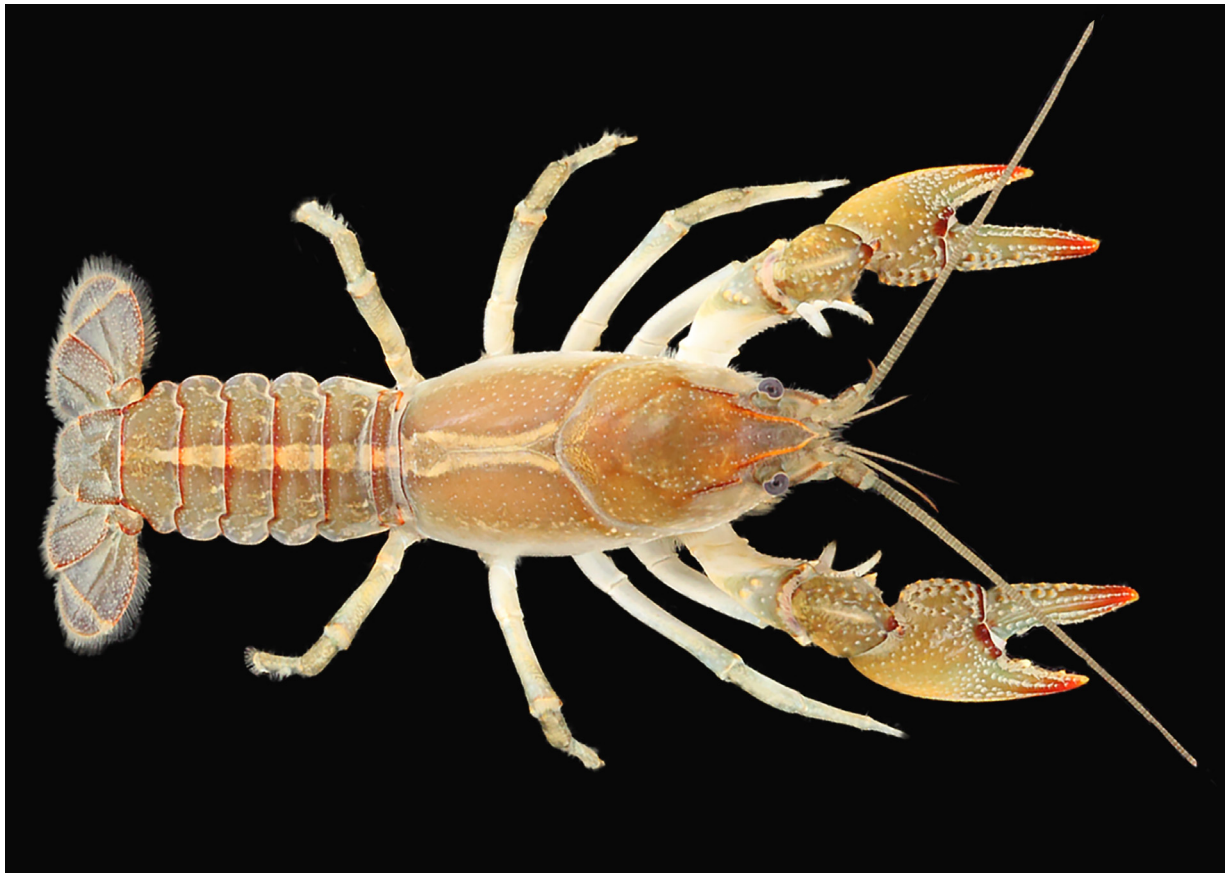
FIGURE 9. Dorsal view of young adult *Lacunicambarus chimera* specimen from Pike County, Indiana (MGG-170812-03). Photo by Mael Glon.

Length of right chela 88% of cephalothorax length; chela width 45% of chela length; palm length 29% of chela length; dactyl length 2.25 times palm length. Dorsomesial margin of palm of chela with 3 rows of tubercles, mesial-most row composed of 7 tubercles running parallel to second row of 7 tubercles, third row running diagonally from mesial base of palm to lateral dactyl articulation comprised of 6 subprobolos tubercles located in shallow dimples, 6 distal tubercles between second and third (diagonal) row. Opposable margin of propodus and dactyl both with rows of 11 tubercles; mesial surface of dactyl studded with 33 tubercles basally, not forming distinct rows, giving way to punctations distally. Mesial surface of cheliped carpus lacking tubercles but with 6 small spines plus 1 large procurved spine near distal margin. Merus ventrolateral margin with row of 7 spines, ventromesial margin with row of 12 spines.

Annulus ventralis (Figure 7K) kite shaped, 1.21 times wider than long, rather deeply embedded in U-shaped sternum, distal half sclerotized, proximal half mildly pliable, with leathery ridge mesially located in cephalic half, distal half of ridge bifurcated, ending in central fossa; tongue extending from sclerotized lingual (sinistral) wall into fossa disappearing under sclerotized supralingual (dextral) wall; lingual, supralingual walls approximately symmetrical, both curved on outer margin; sinus laterally oblong, forming deep fossa on dextral, sinistral sides. Distal margin of annulus ventralis projecting over oblong, approximately symmetrical post-annular sclerite, lacking setae. First pleopods overreach distal edge of annulus ventralis when abdomen flexed.

Morphotypic male, Form II (OSUMC 10651; Figure 7E–F). The morphotypic Form II male differs from the holotype as follows: cephalothorax depth 101% of width (Table 4); maximum width of cephalothorax less than depth at caudodorsal margin of cervical groove (23.41, 23.69 mm, respectively). Areola length 41% of total length of cephalothorax. Antennal scale 2.65 times as long as wide. Posterior margin of cervical groove lined by 7 tubercles, lacking single larger tubercle in cervical groove. Anteroventral branchiostegal region with 18 small tubercles. Abdomen greater in length than cephalothorax, 2.63 times as long as wide.

Length of right chela 74% cephalothorax length, chela width 51% of chela length; palm length 33% of chela length; dactyl length 1.91 times palm length. Dorsomesial margin of palm of chela with 3 rows of tubercles, mesial-most row composed of 8 tubercles running parallel to second row of 5 tubercles, 8 distal tubercles between second and third (diagonal) row. Opposable margin of propodus with row of 10 tubercles, opposable margin of dactyl with row of 12 tubercles. Mesial surface of cheliped carpus with 7 small spines plus 1 large procurved spine near distal margin, lacking tubercles. Merus ventrolateral margin with row of 6 spines, vendromesial margin with row of 12.

Central projection non-corneous and slightly shorter than mesial process, just overreaching umbo near midlength of cephalic surface of gonopod (Figure 7E–F). Mesial process conical, overreaching umbo near midlength of cephalic surface of gonopod, lacking protruding finger. Sinistral gonopod separated from specimen, placed in glass vial inside specimen jar.

Coloration and color pattern. We have observed a great deal of ontogenic variation in the coloration and color pattern of *L. chimera*. Adult specimens resemble the holotype (Figure 6) in having the background of the cephalothorax predominantly olive, yellow green, or golden. The abdomen is similar in color to the cephalothorax, but usually a few shades darker. The proximal half of the uropod is similar in color to the abdomen, but transitions to a soft periwinkle color in the distal half. The chelae are mostly similar in color to the cephalothorax, with the exception of the lateral margins and the tips of the propodus and dactyl, which are apricot orange. The ventral side of the chelae is a similar shade of apricot orange. The proximal portions of the 1st pereipods and the entirety of the 2nd through 5th pereiopods range from a light blue or white to a soft cream in color, as do the ventral sides of the cephalothorax and abdomen. The distal margins of the abdominal somites, telson, and rami, and the dorsal base of the dactyl are highlighted by a deep burgundy color, like that of Pinot Noir. The anterior tip of the postorbital ridge and the rostrum and acumen are highlighted either by this same burgundy color or, in some specimens, by an apricot orange similar to that of the distal portions of the chelae. Prominent tubercles and spines on the merus, carpus, and chelae range from an apricot to burnt orange. A faint longitudinal gladiate (i.e., sword-shaped) stripe highlighting the margins of the areola (i.e., handle), forming a diamond shape at the distal margin of the cephalothorax (i.e., hilt), then tapering and running down the abdomen (i.e., blade) is sometimes faintly present in adult specimens, in which case it is lighter in color to the cephalothorax and abdomen. This stripe is only faintly visible in the holotype.

The coloration of juvenile and young adult specimens is distinct from adults in several ways (Figures 8, 9). The gladiate stripe is much more pronounced in juvenile and young adult specimens and reminiscent of that seen in *L.*

miltus (Fitzpatrick 1978). In these life stages, the stripe ranges from yellow green to orange. Young specimens exhibit mottling on the lateral sides of the cephalothorax and abdomen, of a color matching that of the gladiate stripe. This mottling gradually fades in young adult specimens, but the stripe remains visible in most, but not all, specimens up to a rather large size. The base color of the cephalothorax and abdomen of juveniles and young adults ranges from an olive green to a cider color. Lastly, the tips of dactyl and propodus are typically a red-orange color rather than the apricot color seen in adults.

Size. *Lacunicambarus chimera* is a sizable crayfish. The largest specimen we have measured is the allotypic female, which has a carapace length of 62.68 mm and a total body length of 129.32 mm from the anterior tip of the rostrum to posterior tip of the telson. The largest Form I male that we have measured is the holotype, which has a carapace length of 62.45 mm and a total body length of 121.95 mm. The smallest Form I male that we have measured has a carapace length of 38.90 mm and total body length of 79.05. The mean ± sd carapace lengths and total lengths of all Form I males that we have measured are 53.86 ± 6.01 mm and 106.52 ± 11.87, respectively. The large size of this species is reflected in the size of its burrows, which can have an inside diameter of 7–8 cm and chimneys as high as 30 cm.
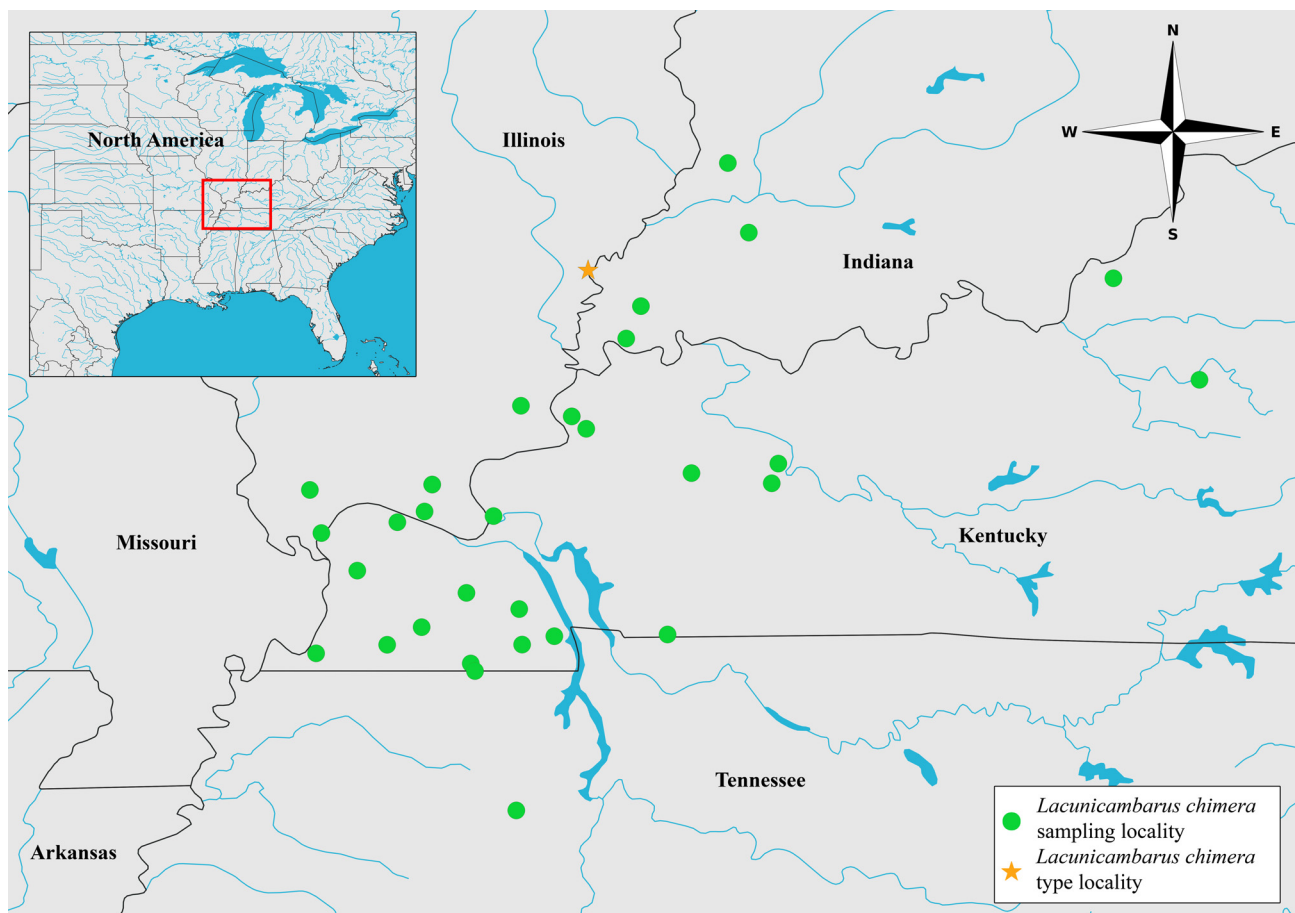

FIGURE 10. Range map of *Lacunicambarus chimera* specimens examined (see Table 1 for details). Green dots indicate collection locality and the orange star represents the type locality of the species.

Variation. *Lacunicambarus chimera* exhibits a moderate amount of variation across its range beyond the color variation mentioned above and normal ontogenic variation (i.e., juveniles having less developed features such as chelae sculpturing and tubercles). A small number of specimens from across the range have a complete row of tubercles consisting of as many as 6 tubercles, located ventrally and parallel to what is typically considered the 1st row of tubercles on the mesial margin of the palm of the chela. Some specimens from Pike County, Indiana have a very rudimentary caudal knob at the caudolateral base of the central projection. The annulus ventralis of some specimens from across the range have small carinas that extend laterally in either direction in ventral view, giving the impression of small wings like those seen on aviator badges. We have occasionally encountered specimens with a single prominent tubercle or, occasionally, a spine, in the cervical groove. This spine or tubercle is far more

conspicuous than the small tubercles that normally line the posterior margin of the cervical groove. Lastly, there is a great deal of variation in the overall shape of the rostrum and acumen, which can be spoon-shaped, sub-trapezoidal, or lanceolate. The rostral margins are also quite variable and range from perfectly straight to slightly concave. As far as we can tell, none of this variation corresponds to sex, age, or geography.

Disposition of Types. The holotype, morphotype, and allotype have been deposited in the OSUMC (OSUMC 10650–10652). Paratypes have been deposited in the USNM (USNM 1480292–1480294).
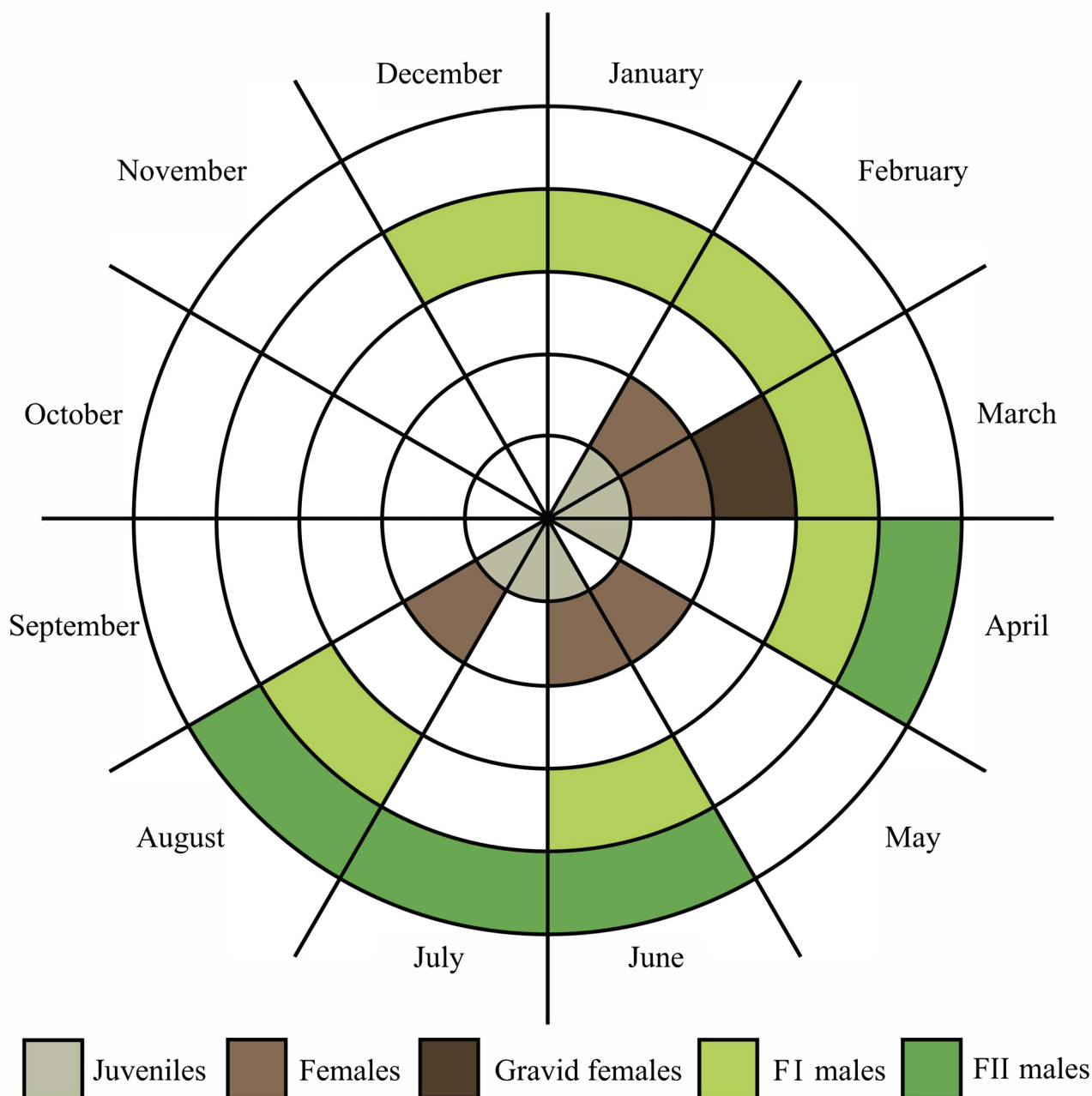

FIGURE 11. Sunburst chart adapted from Miller *et al.* (2014) showing occurrences of different life history stages (represented by different colors) by month in our specimens examined. Abbreviations: FI, Form I; FII, Form II.

Type Locality. We excavated the holotype and morphotype from burrows in a roadside ditch on the east side of Illinois Route 1 (Court Street) approximately 150 m north of the Illinois Route 1 intersection with County Rd 2450 N, 2.4 kilometers south of Grayville in White County, Illinois (38.23870° N, 87.99885° W). This ditch had

been lined with large rocks, likely to prevent erosion, but still sustained a healthy population of *L. chimera* in burrows with characteristically large chimneys at the time of sampling in 2018. We dug the allotype from a burrow in a roadside ditch on the southeast corner of the intersection of Kentucky 109 and Press Road, approximately 2 km west of Sturgis in Union County, Kentucky (37.550308° N, 88.006743° W). This ditch was shallow and mostly surrounded by mown grass dotted with crayfish chimneys at the mouths of shallow burrows at the time of sampling in 2017.

TABLE 4. Measurements (mm) of holotype, allotype, and morphotype of *Lacunicambarus chimera* **sp. nov.** (OSUMC 10650–10652).

Character	Holotype	Allotype	Morphotype
Carapace:			
Depth	29.73	32.65	23.69
Width	31.2	30.91	23.41
Length	62.45	62.68	46.59
Areola:			
Length	28.21	25.76	19.33
Rostrum:			
Width at eyes	7.18	7.02	5.24
Length	9.68	9.77	6.88
Postorbital ridge:			
Width	11.36	12.08	9.18
Chela (right):			
Length of propodus	64.38	55.24	34.66
Length of palm	20.03	15.95	11.47
Width of palm	28.18	24.82	17.56
Length of dactyl	42.39	35.96	21.91
Abdomen:			
Length	59.5	66.64	47.36
Width	23.82	31.91	18.03
Gonopod:			
Length	15.07	NA	9.34
Width at umbo	4.01	NA	2.48
Annulus ventralis:			
Length	NA	5.75	NA
Width	NA	6.45	NA
Antennal scale:			
Length	6.95	8.28	6.07
Width	2.61	3.22	2.29

Range. The majority of our collections of this species are from the Ohio River Basin in southern Indiana and Illinois and western Kentucky (Figure 10). However, we have also collected *L. chimera* in the Lower Mississippi River and Tennessee River Basins in western Kentucky and Tennessee. Lastly, we have a single collection from the Upper Mississippi River Basin in Alexander County, Illinois. The range of this species, while bounded by the Mississippi River in the west, does not seem to correspond with any particular contemporary drainage basin. Likewise, this species' range does not seem to correspond with any particular ecoregion, extending over parts of the Interior River Valleys and Hills, Interior Plateau, Southeastern Plains, and Mississippi Valley Loess Plains (Wiken *et al.* 2011). This general range may suggest that this species is capable of dispersing via large streams and

rivers like other species in this genus and is therefore not restricted by drainage basin boundaries (Helms *et al.* 2013; Miller *et al.* 2014; Glon *et al.* 2018). Alternatively, this species' contemporary range may be a remnant of a paleodrainage, as it corresponds well with the pre-Holocene Old Ohio River whose flow was altered as glaciers advanced southward during the Pleistocene (Strange & Burr 1987; Kozak *et al.* 2006).

Specimens Examined. We examined a total of 143 specimens from 24 counties in four states. See Table 1 for specific information on these specimens.

Conservation status. This species has a fairly large range and is common in appropriate habitat within that range. It seems fairly tolerant of anthropogenic habitat alterations, as evidenced by its success colonizing roadside ditches and artificial ponds. We suggest that it be considered Currently Stable following the American Fisheries Society's Endangered Species Crayfish Subcommittee criteria (Taylor *et al.* 2007) and of Least Concern following the IUCN criteria (IUCN 2001), but also recommend that potential threats specific to this and other burrowing species be explicitly examined.
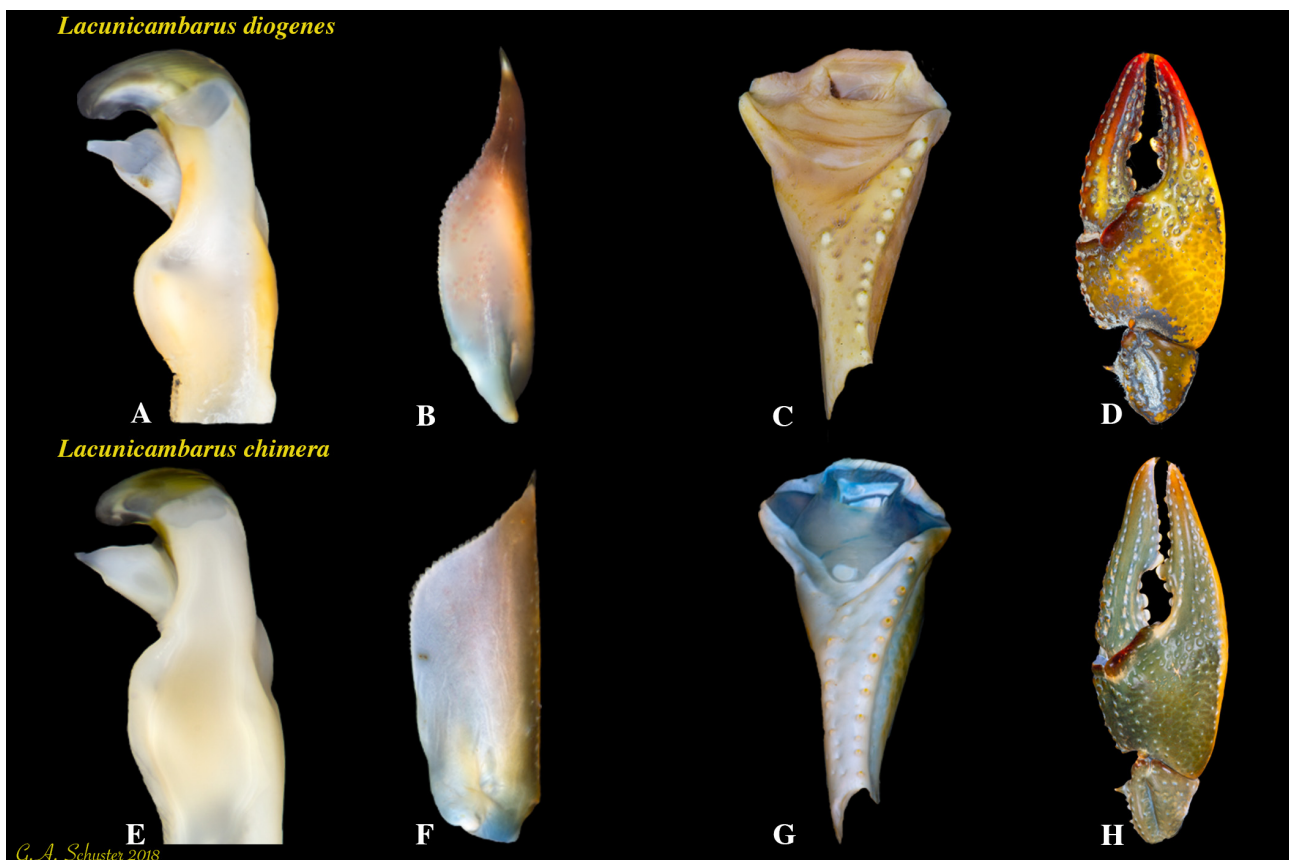

FIGURE 12. From left to right: lateral view of the Form I gonopod, dorsal view of the antennal scale, ventral view of the merus, and dorsal view of the chela of *Lacunicambarus diogenes* (A–D) and *L. chimera* (E-H), respectively. Images A and D from *L. diogenes* neotype (USNM 1498707); B from *L. diogenes* representative Form II male (USNM 1498709); C from Form I specimen from Virginia (USNM 129925). Images E, G and H from *L. chimera* holotype (OSUMC 10650), F from *L. chimera* morphotype (OSUMC 10651).

Life History Notes. We did not explicitly focus on gathering life history data during this study, so our inferences may require revision after a more targeted life history study. *Lacunicambarus chimera* seems to follow the general life histories of the family Cambaridae and of other *Lacunicambarus* species (Hobbs III 2001; Thoma *et al.* 2005; Miller *et al.* 2014; Figure 11). Specifically, our data suggest that most males are in Form I during winter and early spring, which coincides with mating. Some of these males then molt into Form II in late spring or early summer and remain in this Form throughout most of the summer. However, we also found several Form I males during the summer, perhaps because larger males grow more slowly and therefore molt less frequently than smaller conspecifics. It is unclear exactly when males molt back from Form II to Form I because we do not have data for September, October or November, but two Form II specimens that we captured in July 2018 and kept in aquaria

molted to Form I in late August of the same year. We have limited sampling of females in fall and winter and therefore do not have any data on when they may be in glair; however, we examined ovigerous female specimens collected in March, suggesting that they had mated in fall or early winter. We found juvenile specimens from February to August, which further suggests that mating takes place in fall or winter, with eggs hatching in Spring.

We can only speculate about the lifespan of this species. Specimens we have kept in captivity do not seem to grow particularly fast relative to other species, suggesting that large specimens must be quite old. One of the authors (RFT) collected a gravid female of what we now recognize to be *L. chimera* from Gibson County, Indiana on March 23rd, 2001. RFT raised the progeny that hatched from this female's eggs in captivity. Most did not survive more than a few years, but a single individual survived in captivity until January 28th, 2017, confirming that this species has a very high longevity potential, at least in captivity.

Ecological Notes. As mentioned above, *L. chimera* is a primary burrowing crayfish species. Like other *Lacunicambarus* species, *L. chimera* is commonly dug from burrows in fine-grained soils along the floodplains of streams and rivers and in roadside ditches. We have also collected this species in burrows on the banks of manmade ponds and in ditches that were lined with large stones. The chimneys at the mouths of *L. chimera* burrows are often large and conspicuous, attaining heights of 30 cm or more. These burrows, like those of other primary burrowing crayfishes, provide habitat for many other organisms (e.g., Creaser 1931; Pintor & Soluk 2006; Thoma & Armitage 2008). Glon & Thoma (2017) specifically documented the use of *L. chimera* burrows as brooding burrows by eastern cicada killer wasps in Pike County, Indiana.

Little is known about the ecology of *L. chimera* in situ, but specimens which we have kept in laboratory aquariums have readily consumed a variety of aquarium fish foods, snails, earth worms, and leaf litter from streams, suggesting that this species is an opportunistic omnivore. These specimens were mostly active at night, when they foraged around their enclosures. During the day, they rested inside of artificial burrows made from PVC pipes, occasionally twitching their antennae in response to stimuli. They did not appear to be particularly aggressive, compared to other crayfish species.

Updated key to *Lacunicambarus*

The following key is an update of the *Lacunicambarus* key presented in Glon *et al.* (2018) and is based on morphological characters found on adult Form I male specimens.

1. Median spine on mesial ramus of uropod overreaching caudal margin of ramus. . . . *Lacunicambarus acanthura* (Hobbs 1981)
- Median spine on mesial ramus of uropod not overreaching caudal margin of ramus 2
2(1). Dorsomesial margin of palm of chela with two parallel rows of well-developed tubercles, usually numbering 6–8 each, plus a third row running diagonally from mesial base of palm to lateral dactyl articulation, additional scattered tubercles usually present between second and third rows 3
- Dorsomesial margin of palm of chela with dorsomesial 1/4–1/3 studded with tubercles not forming distinct rows 6
3(2). Form I male gonopod with pronounced subapical notch on central projection, caudal knob present at caudolateral base of the central projection; rostrum narrow with sides strongly concave, forming hourglass shape; abdomen reduced in width. 4
- Form I male gonopod lacking or with very weak subapical notch on central projection, caudal knob lacking or rudimentary at caudolateral base of the central projection; rostrum broad with sides straight or weakly concave; abdomen not reduced in width 5
4(3). Cephalic lobe of epistome apically truncate; life colors include single wide longitudinal stripe on dorsal side of abdomen . . . . *Lacunicambarus miltus*
- Cephalic lobe of epistome rounded or subtriangular; life colors include three brightly colored longitudinal stripes on dorsal side of abdomen . . . . *Lacunicambarus ludovicianus* (Faxon 1884)
5(3). Spines on ventrolateral row of merus ranging from 0–4 (mean ± sd: 2 ± 1); antennal scale narrow (length/width range 2.68–3.67, mean ± sd: 3.00 ± 0.19) with long, curved spine; longitudinal stripes on dorsal side of abdomen never present (Figure 12) . . . . *Lacunicambarus diogenes*
- Spines on ventrolateral row of merus ranging from 2–9 (mean ± sd: 5 ± 2); antennal scale wide (length/width range 2.41–3.35, mean ± sd: 2.80 ± 0.18) with short, straight spine; single longitudinal stripe on dorsal side of abdomen usually present (Figure 12) . . . . *Lacunicambarus chimera*
6(2). Rostrum strongly deflected; life color of body greenish, with red or orange highlights and blue hues on the dactyl and distal portion of the chelae . . . . *Lacunicambarus polychromatus* (Thoma *et al.* 2005)
- Rostrum weakly deflected; life color of body dark brown to olive, sometimes with orange highlights on rostrum and tips of chelae. . . . . *Lacunicambarus thomai* (Jezerinac 1993)

Crayfish Associates. We collected the following primary and secondary-burrowing crayfishes from burrows at sites where we found *L. chimera*: *Creaserinus fodiens* (Cottle 1863), *C. hortoni* (Hobbs & Fitzpatrick 1970), *Faxonius immunis* (Hagen 1870), *L. ludovicianus*, *L. polychromatus*, *L.* aff. *polychromatus*, *Procambarus acutus* (Girard 1852), *P. clarkii* (Girard 1852), *P. gracilis* (Bundy in Forbes 1876) and *P. viaeviridis* (Faxon 1914). While sampling for *L. chimera*, we focused primarily on sampling for burrowing crayfishes and therefore do not have records of the tertiary-burrowing crayfishes that undoubtedly inhabit open water adjacent to *L. chimera* burrows.

Etymology. Our choice of the species epithet "*chimera*" stems from our first encounter with this species. The first specimens that we caught were freshly molted young adults (approximately 30 mm CL). These specimens bore a bright longitudinal gladiate stripe reminiscent of the stripe in *L. ludovicianus*, *L. miltus*, and some populations of *L. polychromatus*. The bright colors on these specimens were similar to those found in *L. polychromatus*, and the general shape of these specimens was reminiscent of *L. diogenes*. These features made *L. chimera* appear to be a chimera of multiple *Lacunicambarus* species. To honor the nickname given to this species when it was first discovered by Ray Jezerinac and Whitney Stocker, and also as a reference to its impressive size, we suggest the common name "Crawzilla Crawdad."

References

Ainscough, B.J., Breinholt, J.W., Robison, H.W. & Crandall, K.A. (2013) Molecular phylogenetics of the burrowing crayfish genus *Fallicambarus* (Decapoda: Cambaridae). *Zoologica Scripta*, 42, 306–316.
https://doi.org/10.1111/zsc.12006

Beck, M.W. (2018) *ggord: Ordination plots with ggplot2. R package version 1.1.1*. [software]

Brown, P.L. (1955) *The biology of the crayfishes of central and southeastern Illinois*. Doctoral dissertation, University of Illinois at Urbana-Champaign, Champaign, Illinois, 165 pp.

Bouchard, R.W. (1972) A contribution to the knowledge of Tennessee crayfish. Doctoral dissertation, University of Tennessee, Knoxville, Tennessee, 113 pp.

Bouchard, R.W. (1974) Crayfishes of the Nashville Basin, Tennessee, Alabama and Kentucky (Decapoda, Astacidae). *The Association of Southeastern Biologists Bulletin*, 21, 41.

Chernomor, O., von Haeseler, A. & Minh, B.Q. (2016) Terrace aware data structure for phylogenomic inference from supermatrices. *Systematic Biology*, 65, 997–1008.
https://doi.org/10.1093/sysbio/syw037

Crandall, K.A. & De Grave, S. (2017) An updated classification of the freshwater crayfishes (Decapoda: Astacidea) of the world, with a complete species list. *Journal of Crustacean Biology*, 37, 615–653.
https://doi.org/10.1093/jcbiol/rux070

Creaser, E.P. (1931) Some cohabitants of burrowing crayfish. *Ecology*, 12, 243–244.
https://doi.org/10.2307/1932946

Cottle, T.J. (1863) On the two species of *Astacus* found in Upper Canada. *The Canadian Journal of Industry, Science, and Art*, New Series, 8, 216–219.

Darriba, D., Taboada, G.L., Doallo, R. & Posada, D. (2012) jModelTest 2: more models, new heuristics and parallel computing. *Nature Methods*, 9, 772.
https://doi.org/10.1038/nmeth.2109

Eberly, W.R. (1954) Summary of the distribution of Indiana crayfishes, including new state and county records. *Proceedings of the Indiana Academy of Science*, 64, 281–283.

Edgar, R.C. (2004) MUSCLE: multiple sequence alignment with high accuracy and high throughput. *Nucleic Acids Research*, 32, 1792–1797.
https://doi.org/10.1093/nar/gkh340

Erichson, W.F. (1846) Uebersicht der Arten der Gattung *Astacus*. *Archiv für Naturgeschichte*, 12, 86–103.

Faxon, W. (1884) Descriptions of new species of *Cambarus*, to which is added a synonymical list of the known species of *Cambarus* and *Astacus*. *Proceedings of the American Academy of Arts and Sciences*, 20, 107–158. https://doi.org/10.2307/25138768

Faxon, W. (1885) A revision of the Astacidae Part I. The genera *Cambarus* and *Astacus*. *Memoirs of the Museum of Comparative Zoology at Harvard College*, 10, 1–186.

Faxon, W. (1914) Notes on the crayfishes in the United States National Museum and the Museum of Comparative Zoology with descriptions of new species and subspecies to which is appended a catalogue of the known species and subspecies. *Memoirs of the Museum of Comparative Zoology at Harvard College*, 40, 352–427.

Fetzner Junior, J.W. & Taylor, C.A. (2018) Two new species of freshwater crayfish of the genus *Faxonius* (Decapoda: Cambaridae) from the Ozark Highlands of Arkansas and Missouri. *Zootaxa*, 4399 (4), 491–520. https://doi.org/10.11646/zootaxa.4399.4.2

Fitzpatrick, J.F. Jr. (1978) A new burrowing crawfish of the genus *Cambarus* from Southwest Alabama (Decapoda, Cambaridae). *Proceedings of the Biological Society of Washington*, 91, 748–755.

Forbes, S.A. (1876) List of Illinois Crustacea, with descriptions of new species. *Bulletin of the Illinois State Laboratory of Natural History*, 1, 3–25.

Girard, C. (1852) A revision of the North American Astaci, with observations on their habits and geographical distribution. *Proceedings of the Academy of Natural Sciences of Philadelphia*, 6, 87–91.

Glon, M.G. & Thoma, R.F. (2017) An observation of the use of devil crayfish (*Cambarus* cf. *diogenes*) burrows as brooding habitat by eastern cicada killer wasps (*Sphecius speciosus*). *Freshwater Crayfish*, 23, 55–57.

Glon, M.G., Thoma, R.F., Taylor, C.A., Daly, M. & Freudenstein, J.V. (2018) Molecular phylogenetic analysis of the devil crayfish group, with elevation of *Lacunicambarus* Hobbs, 1969 to generic rank and a redescription of the devil crayfish, *Lacunicambarus diogenes* (Girard, 1852) comb. nov. (Decapoda: Astacoidea: Cambaridae). *Journal of Crustacean Biology*, 38, 600–613. https://doi.org/10.1093/jcbiol/ruy057

Guindon, S. & Gascuel, O. (2003) A simple, fast, and accurate algorithm to estimate large phylogenies by maximum likelihood. *Systematic Biology*, 52, 696–704. https://doi.org/10.1080/10635150390235520

Hagen, H.A. (1870) Monograph of the North American Astacidae. *Illustrated Catalogue of the Museum of Comparative Zoology at Harvard College*, 3, 1–109.

Hay, W.P. (1895) The crawfishes of the state of Indiana. *20th Annual Report of the Indiana Department of Geology and Natural Resources*, 1895, 475–507.

Helms, B., Budnick, W., Pecora, P., Skipper, J., Kosnicki, E., Feminella, J. & Stoeckel, J. (2013) The influence of soil type, congeneric cues, and floodplain connectivity on the local distribution of the devil crayfish (*Cambarus diogenes* Girard). *Freshwater Science*, 32, 1333–1344. https://doi.org/10.1899/12-160.1

Hobbs Junior, H.H. (1969) On the distribution and phylogeny of the crayfish genus *Cambarus*. *The distributional history of the biota of the southern Appalachians. Part I: Invertebrates. Research Division Monograph*, 1, 93–178.

Hobbs Junior, H.H. (1974) A Checklist of the North and Middle American Crayfishes (Decapoda: Astacidae and Cambaridae). *Smithsonian Contributions to Zoology*, 166, 1–161. https://doi.org/10.5479/si.00810282.166

Hobbs Junior, H.H. (1981) The crayfishes of Georgia. *Smithsonian Contributions to Zoology*, 318, 1–549. https://doi.org/10.5479/si.00810282.318

Hobbs Junior, H.H. (1989) An illustrated checklist of the American crayfishes (Decapoda: Astacidae, Cambaridae and Parastacidae). *Smithsonian Contributions to Zoology*, 480, 1–236. https://doi.org/10.5479/si.00810282.480

Hobbs Junior, H.H. & Fitzpatrick, J.F. Jr. (1970) A new crayfish of the genus *Fallicambarus* from Tennessee (Decapoda, Astacidae). *Proceedings of the Biological Society of Washington*, 82, 829–836.

Hobbs III, H.H. (2001) Decapoda. *In*: Thorpe, J.J. & Covich, A.P. (Eds.), *Ecology and Classification of North American Freshwater Invertebrates*. Academic Press, San Diego, California, pp. 955–1001. https://doi.org/10.1016/B978-012690647-9/50024-7

Huelsenbeck, J.P. & Ronquist, F. (2001) MRBAYES: Bayesian inference of phylogenetic trees. *Bioinformatics*, 17, 754–755. https://doi.org/10.1093/bioinformatics/17.8.754

Jezerinac, R.F. (1993) A new subgenus and species of crayfish (Decapoda: Cambaridae) of the genus *Cambarus*, with an amended description of the subgenus *Lacunicambarus*. *Proceedings of the Biological Society of Washington*, 106, 532–544.

Kearse, M., Moir, R., Wilson, A., Stones-Havas, S., Cheung, M., Sturrock, S., Buxton, S., Cooper, A., Markowitz, S., Duran, C., Thierer, T., Ashton, B., Mentjies, P. & Drummond, A. (2012) Geneious Basic: an integrated and extendable desktop software platform for the organization and analysis of sequence data. *Bioinformatics*, 28, 1647–1649. https://doi.org/10.1093/bioinformatics/bts199

Kozak, K.H., Blaine, R.A. & Larson, A. (2006) Gene lineages and eastern North American palaeodrainage basins: phylogeography and speciation in salamanders of the *Eurycea bislineata* species complex. *Molecular Ecology*, 15, 191–

207.
https://doi.org/10.1111/j.1365-294X.2005.02757.x

Loughman, Z.J. & Simon, T.P. (2011) Zoogeography, taxonomy, and conservation of West Virginia's Ohio River floodplain crayfishes (Decapoda, Cambaridae). *ZooKeys*, 74, 1–78.
https://doi.org/10.3897/zookeys.74.808

Loughman, Z.J., Henkanaththegedara, S.M., Fetzner Junior, J.W. & Thoma, R.F. (2017) A case of Appalachian endemism: Revision of the *Cambarus robustus* complex (Decapoda: Cambaridae) in the Kentucky and Licking River basins of Kentucky, USA, with the description of three new species. *Zootaxa*, 4269 (4), 460–494.
https://doi.org/10.11646/zootaxa.4269.4.4

Loughman, Z.J. & Williams, B.W. (2018) *Cambarus polypilosus*, a new species of stream-dwelling crayfish (Decapoda: Cambaridae) from the Western Highland Rim of Tennessee, USA. *Zootaxa*, 4403 (1), 171–185.
https://doi.org/10.11646/zootaxa.4403.1.10

Marlow, G. (1960) The subspecies of *Cambarus diogenes*. *American Midland Naturalist*, 64, 229–250.
https://doi.org/10.2307/2422905

McCune, B., Grace, J.B. & Urban, D.L. (2002) *Analysis of ecological communities*. MjM software design, Gleneden Beach, Oregon, 300 pp.

Miller, J.M., Niraula, B.B., Reátegui-Zirena, E.G. & Stewart, P.M. (2014) Life history and physical observations of primary burrowing crayfish (Decapoda: Cambaridae) *Cambarus* (*Lacunicambarus*) *diogenes* and *Cambarus* (*Tubericambarus*) *polychromatus*. *Journal of Crustacean Biology*, 34, 15–24.
https://doi.org/10.1163/1937240X-00002199

Nguyen, L.T., Schmidt, H.A., von Haeseler, A. & Minh, B.Q. (2014) IQ-TREE: a fast and effective stochastic algorithm for estimating maximum-likelihood phylogenies. *Molecular Biology and Evolution*, 32, 268–274.
https://doi.org/10.1093/molbev/msu300

Ortmann, A.E. (1905) The mutual affinities of the species of the genus *Cambarus*, and their dispersal over the United States. *Proceedings of the American Philosophical Society*, 44, 91–136.
https://doi.org/10.5962/bhl.title.16019

Ortmann, A.E. (1906) The crawfishes of the State of Pennsylvania. *Memoirs of the Carnegie Museum*, 2, 343–524.

Oksanen, J., Blanchet, F.G., Friendly, M., Kindt, R., Legendre, P., McGlinn, D., Minchin, P.R., O'Hara, R.B., Simpson, G.L., Solymos, P., Stevens, M.H.H., Szoecs, E. & Wagner, H. (2018) vegan: Community Ecology Package. R package version 2.5-2. Available from: https://CRAN.R-project.org/package=vegan (accessed 11 October 2018)

Page, L.M. (1985) The crayfishes and shrimps (Decapoda) of Illinois. *Illinois Natural History Survey Bulletin*, 33, 335–448.

Page, L.M. & Mottesi, G.B. (1995) The distribution and status of the Indiana crayfish, *Orconectes indianensis*, with comments on the crayfishes of Indiana. *Proceedings of the Indiana Academy of Science*, 104, 103–112.

Pintor, L.M. & Soluk, D.A. (2006) Evaluating the non-consumptive, positive effects of a predator in the persistence of an endangered species. *Biological Conservation*, 130, 584–591.
https://doi.org/10.1016/j.biocon.2006.01.021

R Core Team (2017) R: A language and environment for statistical computing. R Foundation for Statistical Computing, Vienna, Austria. Available from: https://www.R-project.org/ (accessed 11 October, 2018)

Richman, N.I., Bohm, M., Adams, S.B., Alvarez, F., Bergey, E.A., Bunn, J.J., Burnham, Q., Cordeiro, J., Coughran, J., Crandall, K.A., Dawkins, K.L., DiStefano, R.J., Doran, N.E., Edsman, L., Eversole, A.G., Fureder, L., Furse, J.M., Gherardi, F., Hamr, P., Holdich, D.M., Horwitz, P., Johnston, K., Jones, C.M., Jones, J.P., Jones, R.L., Jones, T.G, Kawai, T., Lawler, S., Loïpez-Mejiïa, M., Miller, R.M., Pedraza- Lara, C., Reynolds, J.D., Richardson, A.M., Schultz, M.B., Schuster, G.A., Sibley, P.J., Souty-Grosset, C., Taylor, C.A., Thoma, R.F., Walls, J., Walsh, T.S. & Collen, B. (2015) Multiple drivers of decline in the global status of freshwater crayfish (Decapoda: Astacidea). *Philosophical Transactions of the Royal Society of London B*, 370, 20140060.
https://doi.org/10.1098/rstb.2014.0060

Rhoades, R. (1944) The crayfishes of Kentucky, with notes on variation, distribution and descriptions of new species and subspecies. *The American Midland Naturalist*, 31, 111–149.
https://doi.org/10.2307/2421386

Ronquist, F. & Huelsenbeck, J.P. (2003) MRBAYES 3: Bayesian phylogenetic inference under mixed models. *Bioinformatics*, 19, 1572–1574.
https://doi.org/10.1093/bioinformatics/btg180

Simon, T.P. (2001) Checklist of the crayfish and freshwater shrimp (Decapoda) of Indiana. *Proceedings of the Indiana Academy of Science*, 110, 104–110.

Strange, R.M. & Burr, B.M. (1997) Intraspecific phylogeography of North American highland fishes: a test of the Pleistocene vicariance hypothesis. *Evolution*, 51, 885–897.
https://doi.org/10.1111/j.1558-5646.1997.tb03670.x

Taylor, C.A. & Schuster, G.A. (2004) The crayfishes of Kentucky. Illinois Natural History Survey, Champaign, Illinois, 220 pp.

Taylor, C.A., Schuster, G.A., Cooper, J.E., DiStefano, R.J., Eversole, A.G., Hamr, P., Hobbs III, H.H., Robison, H.W., Skelton, C.E. & Thoma, R.F. (2007) A reassessment of the conservation status of crayfishes of the United States and Canada after 10+ years of increased awareness. *Fisheries*, 32, 372–389.

https://doi.org/10.1577/1548-8446(2007)32[372:AROTCS]2.0.CO;2

Taylor, C.A., Schuster, G.A. & Wylie, D. (2015) Field guide to crayfishes of the Midwest. *Illinois Natural History Survey*. Champaign, Illinois, 164 pp.

Taylor, C.A., Warren Jr., M.L., Fitzpatrick Jr., J.F., Hobbs III, H.H., Jezerinac, R.F., Pflieger, W.L. & Robison, H.W. (1996) Conservation status of crayfishes of the United States and Canada. *Fisheries*, 21, 25–38.
https://doi.org/10.1577/1548-8446(1996)021%3C0025:CSOCOT%3E2.0.CO;2

Thoma, R.F., Jezerinac, R.F. & Simon, T.P. (2005) *Cambarus* (*Tubericambarus*) *polychromatus* (Decapoda: Cambaridae), a new species of crayfish from the United States. *Proceedings of the Biological Society of Washington*, 118, 326–336.
https://doi.org/10.2988/0006-324X(2005)118[326:CTPDCA]2.0.CO;2

Thoma, R.F. & Armitage, B.J. (2008) *Burrowing crayfish of Indiana. Final Report.* Indiana Department of Natural Resources Division of Fish & Wildlife, Wildlife Diversity Section, Indianapolis, Indiana, 226 pp.

Thoma, R.F., Fetzner, J.W. Jr., Stocker, G.W. & Loughman, Z.J. (2016) *Cambarus* (*Jugicambarus*) *adustus*, a new species of crayfish from northeastern Kentucky delimited from the *Cambarus* (*J.*) aff. *dubius* species complex. *Zootaxa*, 4162 (1), 173–187.
https://doi.org/10.11646/zootaxa.4162.1.9

Wickham, H. (2016) *ggplot2: elegant graphics for data analysis*. Springer-Verlag, New York. [software]

Wiken, E., Francisco, J.N. & Glenn, G. (2011) *North American terrestrial ecoregions—Level III*. Commission for Environmental Cooperation, Montreal, 149 pp.